NUREG/CR-4232
LA-10413-MS

Los Alamos National Laboratory is operated by the University of California for the United States Department of Energy under contract W-7405-ENG-36

The Response of Ventilation Dampers to Large Airflow Pulses

Los Alamos Los Alamos National Laboratory
Los Alamos, New Mexico 87545

Edited by Mary C. Timmers, Group Q-6
Prepared by T. M. Glassmire, Group Q-6

NUREG/CR-4232
LA-10413-MS

RD

The Response of Ventilation Dampers to Large Airflow Pulses

W. S. Gregory
P. R. Smith*

Manuscript submitted: April 1985
Date published: April 1985

Prepared for
Transportation and Material Risk Branch
Division of Risk Analysis
Office of Nuclear Regulatory Research
US Nuclear Regulatory Commission
Washington, DC 20555

NRC FIN No. A7028

*Consultant at Los Alamos. New Mexico State University, Las Cruces, NM 88003.

Los Alamos

Los Alamos National Laboratory
Los Alamos, New Mexico 87545

THE RESPONSE OF VENTILATION DAMPERS TO LARGE AIRFLOW PULSES

by

W. S. Gregory and P. R. Smith

ABSTRACT

The results of an experimental program to evaluate the response of ventilation system dampers to simulated tornado transients are reported. Relevant data, such as damper response time, flow rate and pressure drop, and flow/pressure vs blade angle, were obtained, and the response of one tornado protective damper to simulated tornado transients was evaluated. Empirical relationships that will allow the data to be integrated into flow dynamics codes were developed. These flow dynamics codes can be used by safety analysts to predict the response of nuclear facility ventilation systems to tornado depressurizations.

I. INTRODUCTION

Safety analysis reviews for nuclear fuel cycle facilities require evaluating the effect of natural phenomena on facility designs. The potential effect of one type of phenomenon, a tornado, on facility air-cleaning systems can be evaluated using computer codes such as TVENT.[1] TVENT calculates the transient pressures and flows throughout a facility and its ventilation system. However, a code such as TVENT has limitations and depends on empirical response relationships determined from experimental data. Ventilation components such as filters, blowers, and dampers can have significant effects on the flow dynamics of an air-cleaning system.

In this report, we discuss the reponse of ventilation system dampers to simulated tornado-generated transients. Light- and medium-duty ventilation dampers, a backdraft damper, and one tornado protective damper were evaluated. The data needed for integration into flow dynamics computer codes were obtained, and these include reponse time vs flow rate, pressure drop vs blade angle, and pressure drop vs flow rate. These data then were transformed into empirical response relationships. The structural response of the dampers was also studied for various flow transients.

II. DESCRIPTION OF DAMPERS

Dampers are used as valves to obtain desired directions, flows, and pressures within a ventilation system. In conventional air conditioning and ventilating applications, little consideration is given to rigid specifications for the dampers; however, many specifications are considered for nuclear applications. Some of these considerations are

- damper function,
- pressure drop across closed dampers,
- normal blade operating position,
- maximum closing and opening times,
- failure mode and blade position,
- seismic requirements,
- permissible leakage through a closed damper, and
- damper and controller response to pressure and flow transients.

Damper functions include the following.

- Flow control
- Pressure control
- Balancing
- Shutoff
- Isolation
- Backdraft
- Pressure-relief

Depending on its function, a damper may be constructed in several configurations. Opposed- and parallel-blade configurations are discussed in detail below.

In this investigation we had to select representative dampers used in the nuclear industry. We chose to use the type of dampers used in the Los Alamos National Laboratory's plutonium research building as a basis. Although the size of the dampers can vary over a wide range, most of the dampers used in the plutonium research building for pressure balancing and flow control are 0.61 m by 0.61 m (2 ft by 2 ft) in cross section. However, tornado and backdraft dampers can be as large as 3.66 m (12 ft) in diameter. Isolation dampers of this size recently were installed at the Department of Energy's Rocky Flats plant in Denver, Colorado. For our tests, the dampers were approximately 0.61 m by 0.61 m (2 ft by 2 ft) in cross section. Our survey indicated that this size commonly is used, and our blowdown system is limited to this size.

Five devices were tested:

- an opposed-blade, medium-duty damper;
- an opposed-blade, light-duty damper;
- a parallel-blade, light-duty damper;
- a backdraft damper; and
- a tornado damper.

The first four dampers were manufactured by American Warming and Ventilating, Inc. Figures 1 and 2 show the configurations of these dampers. Each has a 57.15- by 57.15-cm (22.5- by 22.5-in.) inside cross section. Alternate blades of the opposed-blade dampers opened in opposite directions, whereas all the blades of the parallel-blade dampers opened in the same direction (Fig. 1). The blades of the backdraft damper also opened in the same direction (Fig. 2). Figure 3 is a photograph of an opposed-blade damper (left) and a parallel-blade damper (right); Fig. 4 is a photograph of a backdraft damper.

The opposed-blade and parallel-blade dampers all were built to allow actuation by pneumatic controllers. However, during the quasi-steady testing of these dampers, their blades were all fixed at the desired angles by clamping the blade-actuating mechanism. In this way, quasi-steady resistance profiles could be obtained for the dampers at fixed blade angles. The backdraft damper was controlled by a weight on a variable-length lever arm. A high-speed motion picture camera was trained on a blade angle dial indicator during transient testing to measure blade angle as a function of time.

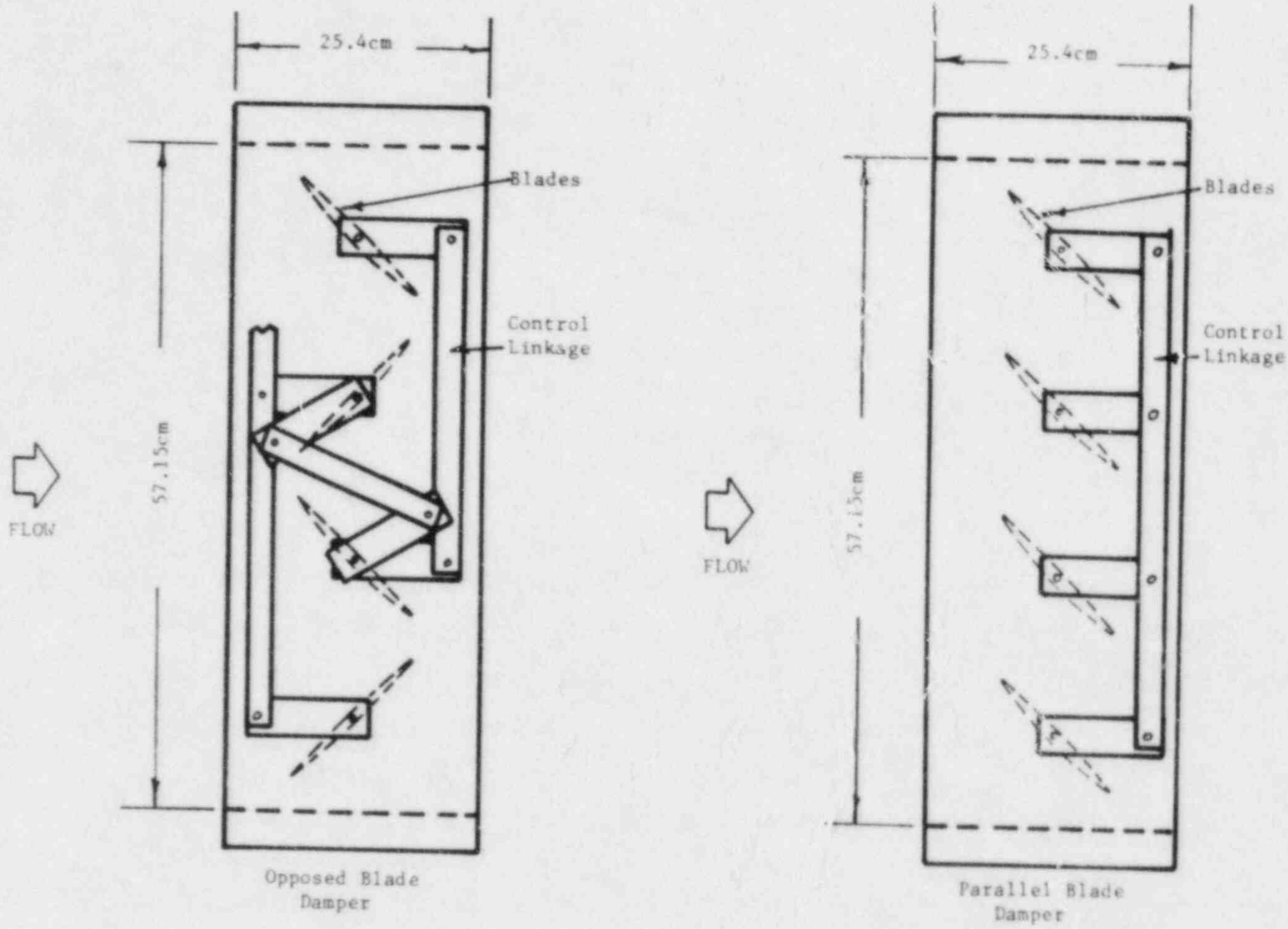

Fig. 1. Side views of the opposed-blade and the parallel-blade dampers.

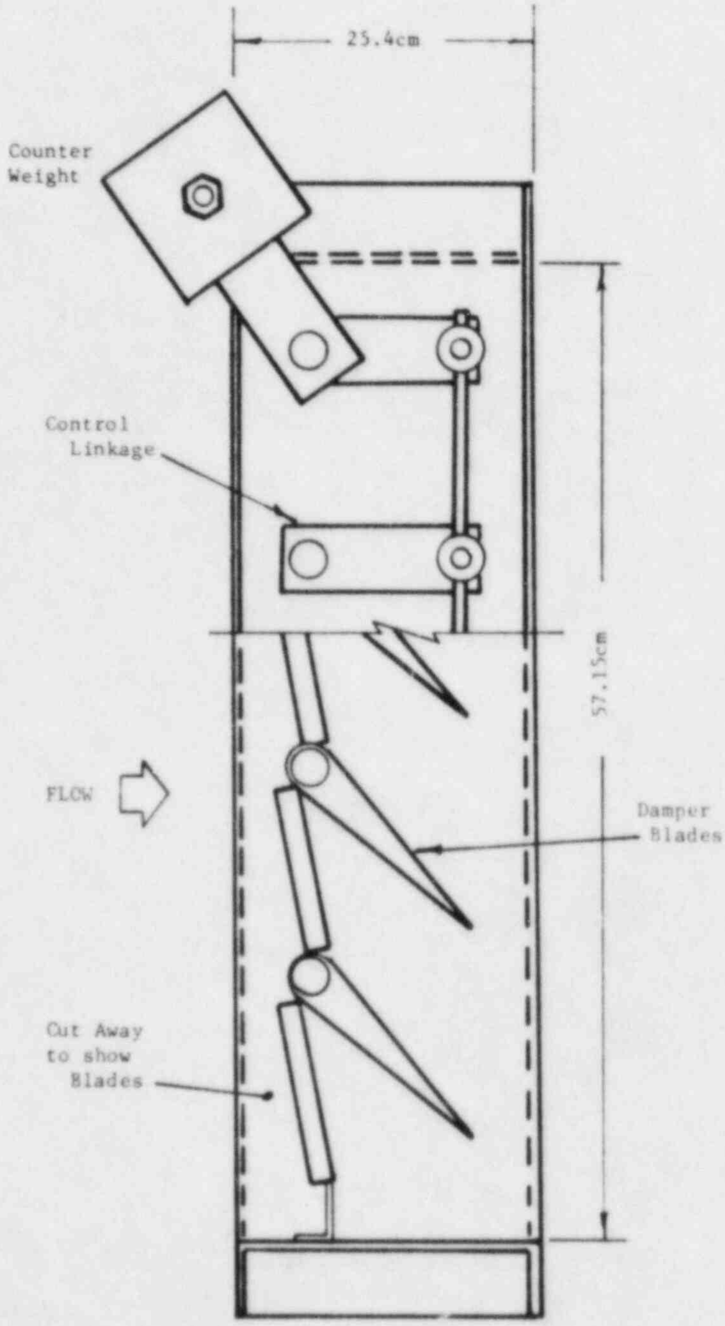

Fig. 2. Side view of backdraft damper.

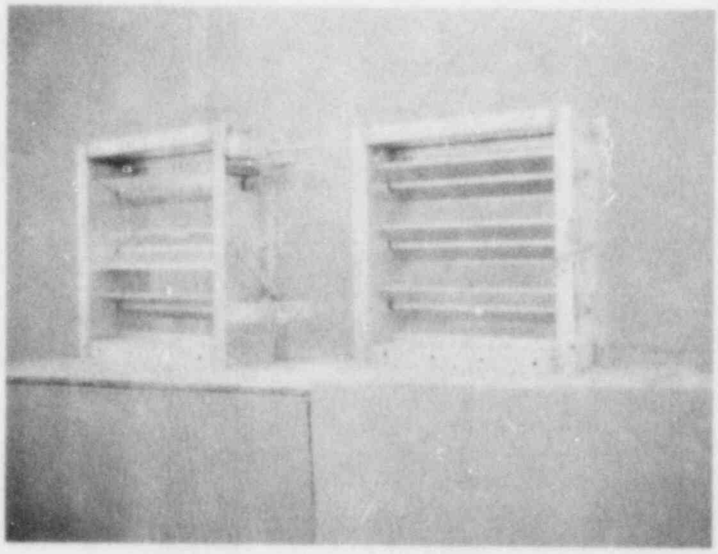

Fig. 3. Opposed-blade (left) and parallel-blade (right) dampers.

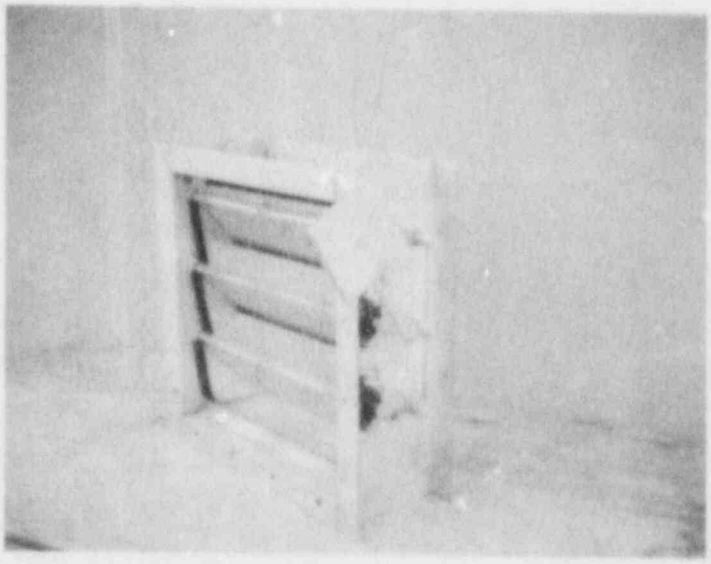

Fig. 4. Backdraft damper.

The tornado damper, which was built by Techno Corporation, has a 50.8- by 71.12-cm (20- by 28-in.) inside cross section, shown in the schematic diagram in Fig. 5. The damper's two valve plates face opposite from the direction in which a tornado pulse is expected. The extension springs hold the valve plates in the open position against normal exhaust flow forces. An increase in flow, such as might be expected from the presence of a tornado inducing a negative pressure downstream of the damper, will cause the plates to close against the spring forces. Return to normal atmospheric conditions allows the springs to reopen the valve plates. Figure 6 is a photograph of the tornado damper.

III. TEST APPARATUS AND PROCEDURES

A. Blowdown System

Figure 7 is a schematic diagram of the blowdown wind tunnel used to simulate a tornado pressure pulse. Air from two large storage tanks is supplied at

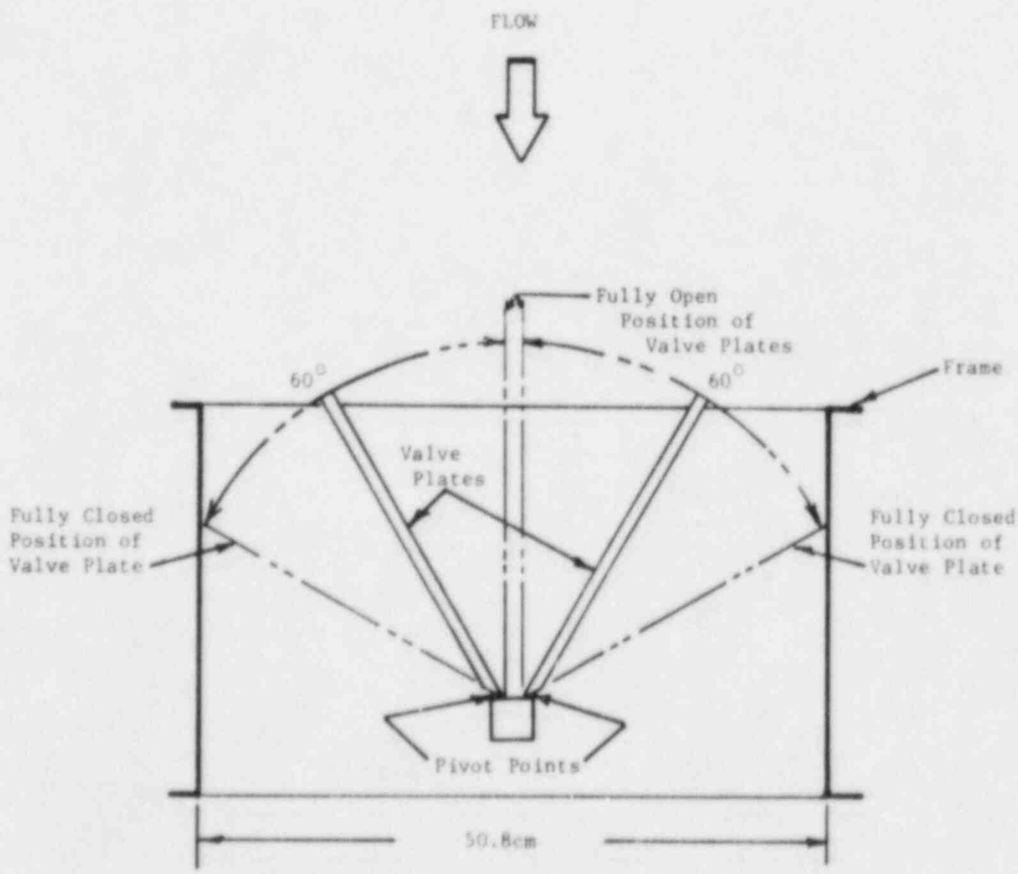

Fig. 5. Top view cut-away of the Techno tornado damper.

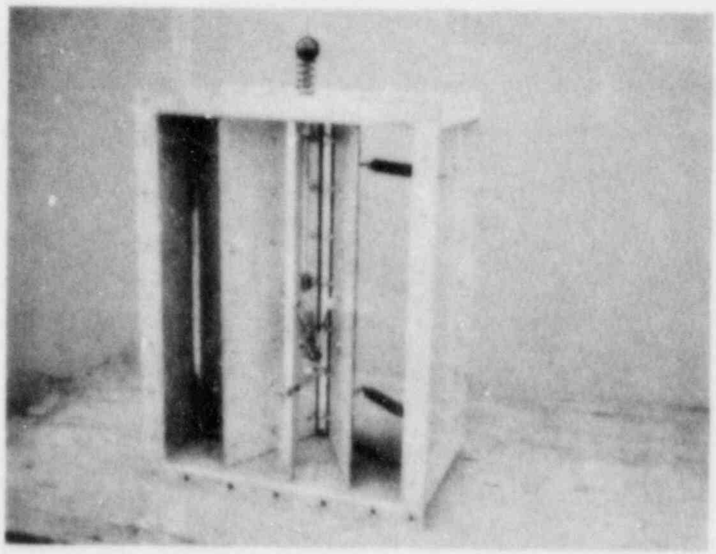

Fig. 6. Techno tornado damper.

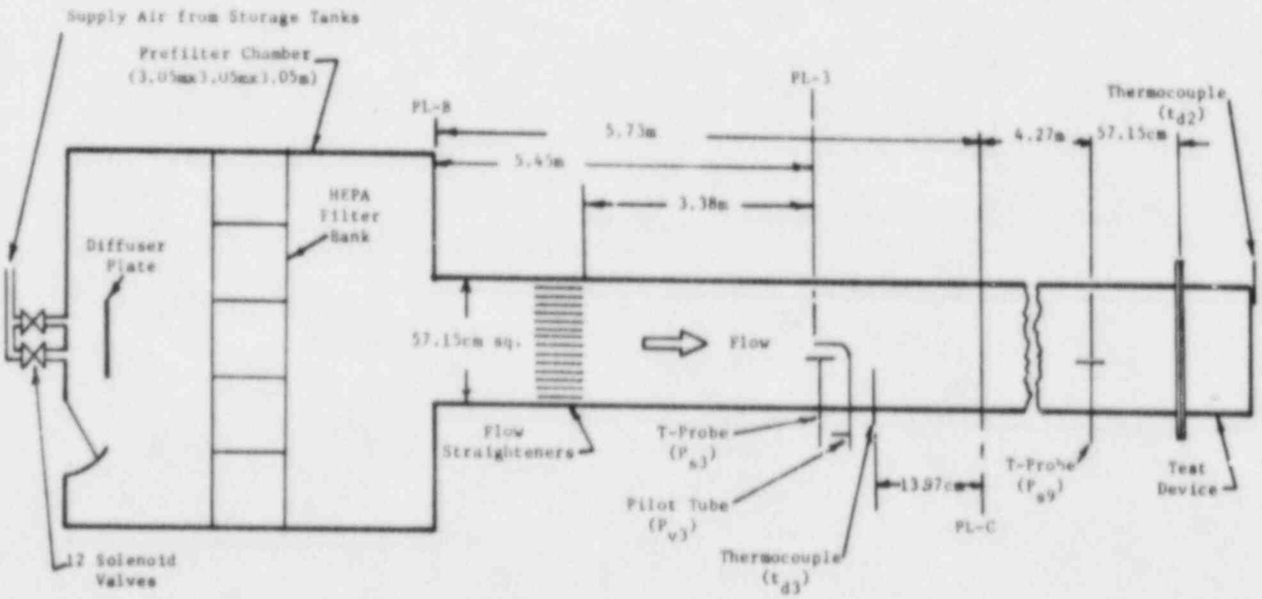

Fig. 7. Blowdown wind tunnel used to simulate tornado pressure pulses.

pressures up to 2760 kPa (400 psig) to 12 sonically limited solenoid valves connected to a 3.05- by 3.05- by 3.05-m (10- by 10- by 10-ft) prefilter chamber. The valves are opened sequentially by an electronic timer in a pattern that can produce a pressure pulse equivalent to the Nuclear Regulatory Commission (NRC) Region I standard tornado (Fig. 8). The tunnel also can be operated in a quasi-steady mode by opening all or some of the valves simultaneously and allowing the storage tank to empty slowly. Various pressure drops across the dampers can be obtained by controlling the initial pressure in the tanks and by the number of valves opened.

The duct of the blowdown wind tunnel is 57.15 by 57.15 cm (22.5 by 22.5 in.) in inside cross section. Transition sections 1.22 m (4 ft) long connect the various dampers to this duct. The flow straighteners and the placement of pressure and temperature probes within the duct conform to the Air Movement and Control Association (AMCA) Standard 500-75 (Ref. 2).

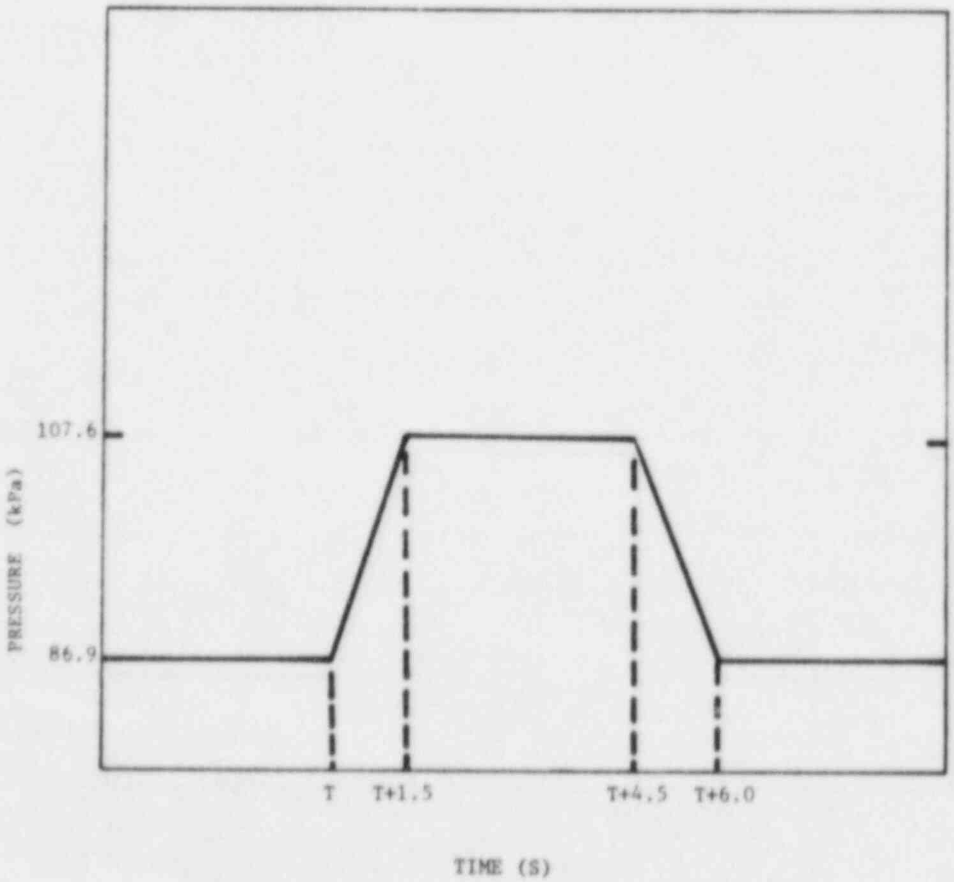

Fig. 8. Simulated Region I tornado pressure pulse.

B. Instrumentation

The locations of the primary instrumentation for the damper tests are shown in Fig. 7. Velocity pressure (P_{v3}) is measured by a centerline pitot tube located 4.84 m (15.875 ft) upstream of the test device. A T-probe (P_{s3}) to measure static pressure and a copper-Constantan thermocouple to measure air temperature (t_{d3}) are also at this location (PL-3). A second T-probe was placed on the centerline of the duct 57.15 cm (22.5 in.) upstream of the test device to measure the static pressure (P_{s9}), which is equivalent to the pressure drop across the device. The pressure-sensing elements used for all three duct pressure measurements were Validyne model DP7 differential pressure transducers with an output voltage range of 0 to 10 V; thermocouple output voltage was in the millivolt range. For both quasi-steady and transient testing, data from these transducers were recorded by a Digital Equipment Corp. (DEC) PDP11/05 digital computer. Other instrumentation included dry and wet bulb thermometers, a mercury barometer, and a Visual Instrumentation Corp. Locam high-speed motion picture camera.

C. Calibration of Instrumentation

The dry and wet bulb thermometers, copper-Constantan thermocouples, and mercury barometer were the primary instruments. The Validyne pressure transducers were calibrated before every test against either a red oil or water manometer. Five pressures between 0 and ~6.9 kPa (1.0 psig) for P_{s3} and P_{s9} and between 0 and ~2.1 kPa (0.3 psig) for P_{v3} were tabulated against the voltage output of the transducers as shown in Table I. The full voltage range of the transducers was used to insure maximum possible accuracy of measurement. A least-squares fit of pressure as a function of voltage then was performed on the PDP11/05 as part of the data acquisition program that output pressure directly in engineering units at the end of each test.

The airflow rate in the duct for each test was determined from a single pitot tube located at the centerline of the duct at PL-3. Calibration of this pitot tube followed AMCA Standard 210-74 (Ref. 3). As shown in Fig. 9, a rake consisting of an array of 16 pitot tubes was placed at PL-3 with the centerline pitot tube. The root-mean-square average of the 16 velocity pressures was compared with the centerline velocity pressure for 5 different flow rates. A least-squares fit of these data gave the relationship between the average velocity pressure and the centerline velocity pressure as

TABLE I

CALIBRATION OF PRESSURE TRANSDUCERS

TEST I.D. BD 97,98

Transducer:	Validyne		Transducer:	Validyne		Transducer:	Validyne	
Quantity:	P_{s9}		Quantity:	P_{s3}		Quantity:	P_{v3}	
Time:	02:00		Time:	02:07		Time:	02:30	
Temperature:	20°C (69.8°F)		Temperature:	22°C (70.6°F)		Temperature:	22°C (70.6°F)	
Manometer (in. R.O.) 0.826	Volts (dc)	Eng. Units (psig)	Manometer (in. R.O.) 0.826	Volts (dc)	Eng. Units (psig)	Manometer (in. R.O.) 0.826	Volts (dc)	Eng. Units (psig)
0.0	0.006	0.0	0.0	0.009	0.0	0.0/20	0.002	0.0
25.0	2.402	0.7475	25.0	2.432	0.7473	0.0/20	0.895	0.0008
50.2	4.794	0.495	50.2	4.839	0.495	2.2/20	0.779	0.0006
75.3	7.063	2.242	75.3	7.097	2.242	3.3/20	2.664	0.0023
000.4	9.504	2.99	000.4	9.498	2.989	4.4/20	3.503	0.0030
* 9.5 Vdc Full Scale *			* 9.5 Vdc Full Scale *			* 3.5 Vdc Full Scale *		

*GAIN = 2.0.

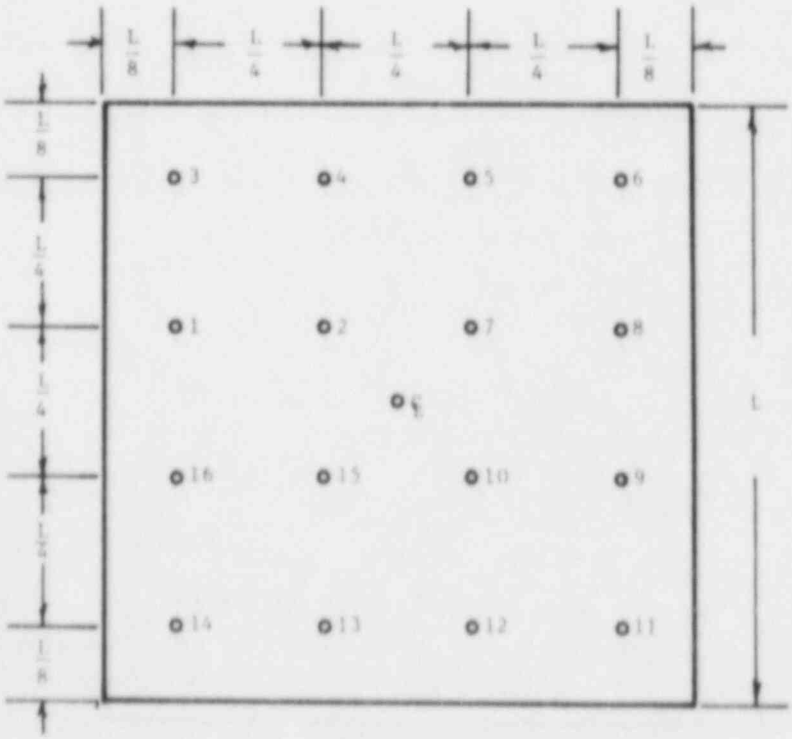

Fig. 9. Pitot rake arrangement for calibration of centerline pitot tube.

$$P_{v3} = 0.831 \times P_{v3c} + 0.001 \quad \text{(in. w.g.)}, \tag{1}$$

in which P_{v3} is the average velocity pressure and P_{v3c} is the centerline velocity pressure.

1. Calculations for Quasi-Steady Tests. The calculations to determine the flow rate and the pressure drop across the dampers were based on AMCA Standard 500-75 (Ref. 2). The equations that follow are taken directly from that publication and therefore are in English engineering units. However, all results presented in this report have been converted to SI units.

The pressure drop across the dampers is calculated as

$$\Delta P = \frac{1}{n}\left(P_{s9\,r}\right) \quad \text{(in. w.g.)}, \tag{2}$$

where P_{s9} is the static pressure at location PL-9 and n is the number of measurements. The average velocity pressure is calculated as

$$\overline{P}_{v3} = \left\{\frac{{}^{\;\;n}_{r\,=\,1}\sqrt{P_{v3\,r}}}{n}\right\}^2 \quad \text{(in. w.g.)}, \tag{3}$$

in which P_{v3} is the average velocity pressure, P_{v3} is the instantaneous velocity pressure, and n is the number of measurements made at location PL-3. The average static pressure is obtained using

$$P_{s3} = \frac{1}{n}\sum\left(P_{s3}\right)_r \quad \text{(in. w.g.)}, \tag{4}$$

where P_{s3} is the average static pressure, P_{s3} is the instantaneous static pressure, and n is the number of measurements made at location PL-3. The average static temperature is found through

$$t_{d3} = \frac{1}{n}\sum(t_{d3})_Y \quad \text{(in. w.g.)}, \tag{5}$$

where t_{d3} is the average static temperature, t_{d3} is the instantaneous static temperature, and n is the number of measurements made at location PL-3.
The local air density is calculated by

$$p_e = (2.96 \times 10^{-4})t^2_{wo} - (1.59 \times 10^{-2})t_{wo} + 0.41 \text{ (in. w.g.)}, \tag{6}$$

in which p_e is an equivalent pressure and t_{wo} is the wet bulb temperature of the atmosphere in degrees Fahrenheit.

$$p_p = p_e - p_b\left(\frac{t_{do} - t_{wo}}{2700}\right) \text{ (in. mercury)}, \tag{7}$$

where p_p is a correction for moisture content, p_b is the barometric pressure read, and t_{do} is the atmospheric dry bulb temperature in degrees Fahrenheit.

$$\rho_o = 70.73 \frac{(p_b - 0.378p_p)}{R(t_{do} + 459.7)} \text{ (pounds-mass per square foot)}, \tag{8}$$

in which ρ_o is the corrected atmospheric density and R is the universal gas constant ($R = 53.35 \text{ ft} \times lb_f/lb_m^oR$).

$$\rho_3 = \rho_o \frac{t_{do} + 459.7}{t_{d3} + 459.7} \frac{p_{s3} + 13.63p_b}{13.63p_b} \text{ (pounds-mass per cubic foot)}, \tag{9}$$

in which ρ_3 is the air density at location PL-3. The quasi-steady velocity is obtained using

$$V_3 = 1096\sqrt{P_{v3}/\rho_3} \quad (\text{ft/min}), \tag{10}$$

in which V_3 is the uniform velocity at location PL-3. The flow rate is calculated as

$$Q_3 = V_3A_3 = 3.515V_3 \quad (\text{ft}^3/\text{min}), \tag{11}$$

where Q_3 is the flow rate and A_3 is the cross-sectional area of the duct at location PL-3.

2. Calculations for Transient Tests. The same equations that were used for the quasi-steady tests are used for the transient tests to calculate ΔP and Q_3, but instantaneous values of the pressures and temperatures are used here rather than the average values.

3. Maximum Expected Error. The maximum expected error in pressure drop across the dampers and in the flow rate is calculated using the least counts below.

Temperature: 0.5°F (thermometers), 0.1°F (thermocouples)
Barometric Pressure: 0.005 in. of mercury
Pressure: 0.03 psi (P_{s3} and P_{s9}), 0.003 psi (P_{v3})

If the foregoing least counts are used in Eqs. (2) through (11), the following results are obtained.

$$\Delta P = \frac{1}{n}\sum(P_{s9})_r \pm 0.82 \quad (\text{in. w.g.}), \text{ and} \tag{12}$$

$$Q_3 = 3.515V_3(1 \pm 0.09) \quad (\text{ft}^3/\text{min}). \tag{13}$$

Thus, the maximum expected error in the pressure drop across the dampers is 0.82 in. w.g. or 0.1 kPa, and the maximum expected error for the flow rate is ~9% of the apparent measured value.

D. Procedures

Each damper test began with the calibration of the pressure transducers as described and by recording the ambient conditions.

1. Quasi-Steady Tests. The quasi-steady tests were run after first charging the storage tanks to ~ 2070 kPa (300 psig). Only the opposedblade and parallel-blade dampers were subjected to these tests. The inlet valves of the prefilter chamber were limited sonically in flow rate, and the flow rate remained relatively constant for several seconds. Low flow rates were obtained by opening only one or two valves. After we recorded the pressure drop, static pressures, velocity pressure, and temperatures, one or two more valves were opened to increase the flow rate. This procedure was continued until all 12 valves were open. Figure 10 is an analog record of the various pressures as a function of time during a typical quasi-steady test.

2. Transient Tests. The sonically limited inlet valves were programmed to open sequentially to produce a pressure pulse across the test device (either the backdraft damper or the tornado damper) that closely approximated a tornado pressure pulse (Fig. 8). Pressure and temperature data were recorded continuously by the digital computer and analog recorder during the test. Figure 11 is a typical analog plot of the pressures during a transient test of the tornado damper. The timing circuit that gained on the valves of the blowdown wind tunnel also started a high-speed motion picture camera that recorded the angle of the valve plates as a function of time. Timing marks on the film were synchronized with timing marks sent to the digital computer and to the analog recorder.

IV. RESULTS

A. Quasi-Steady Tests

Figures 12--14 show the pressure drop through the opposed-blade and parallel-blade dampers as a function of the flow rate of five fixed blade angles. The opposed-blade, medium-duty damper results are shown in Fig. 12; the opposed-blade, light-duty damper results are shown in Fig. 13; and the parallel-blade, light-duty damper results are shown in Fig. 14. Each data point on these curves represents one quasi-steady test condition.

At the wide-open position (that is, a blade angle of 90°), there is very little pressure drop through the dampers for all three types even at high flow rates. Also, the curve of pressure drop as a function of flow rate at a 90° blade angle is virtually identical for all three types of dampers. For the

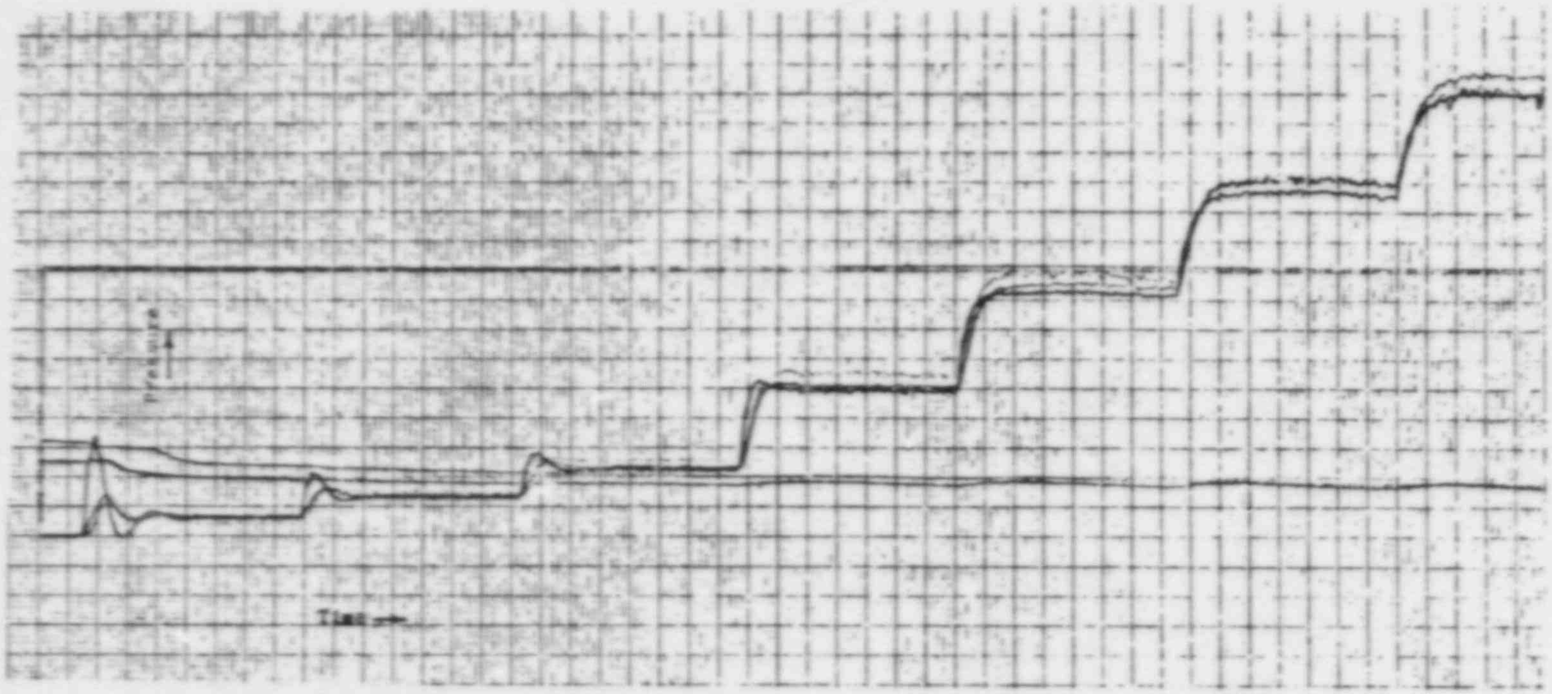

Fig. 10. Analog record of quasi-steady pressure steps.

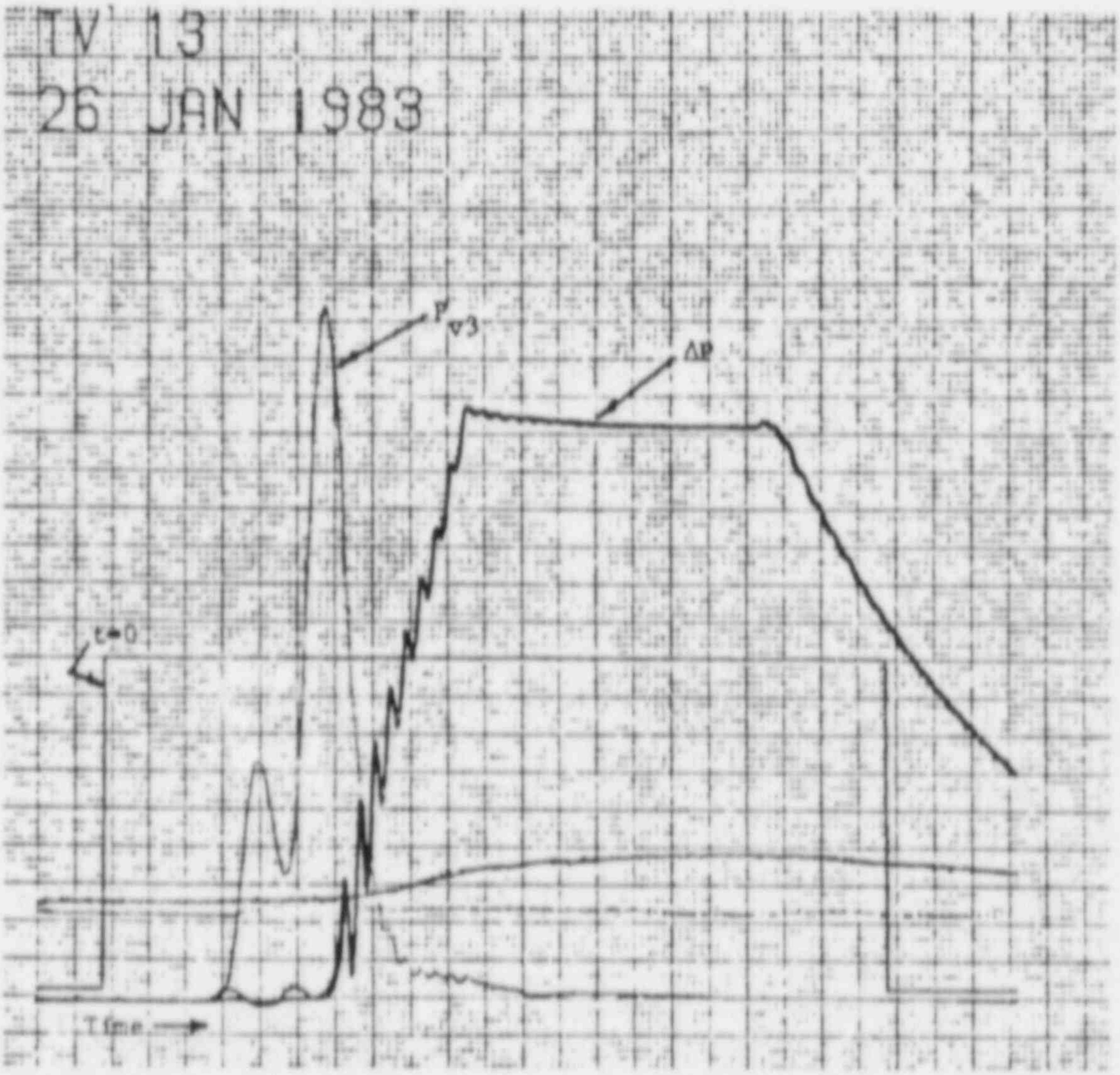

Fig. 11. Analog record of transient response of the Techno tornado damper.

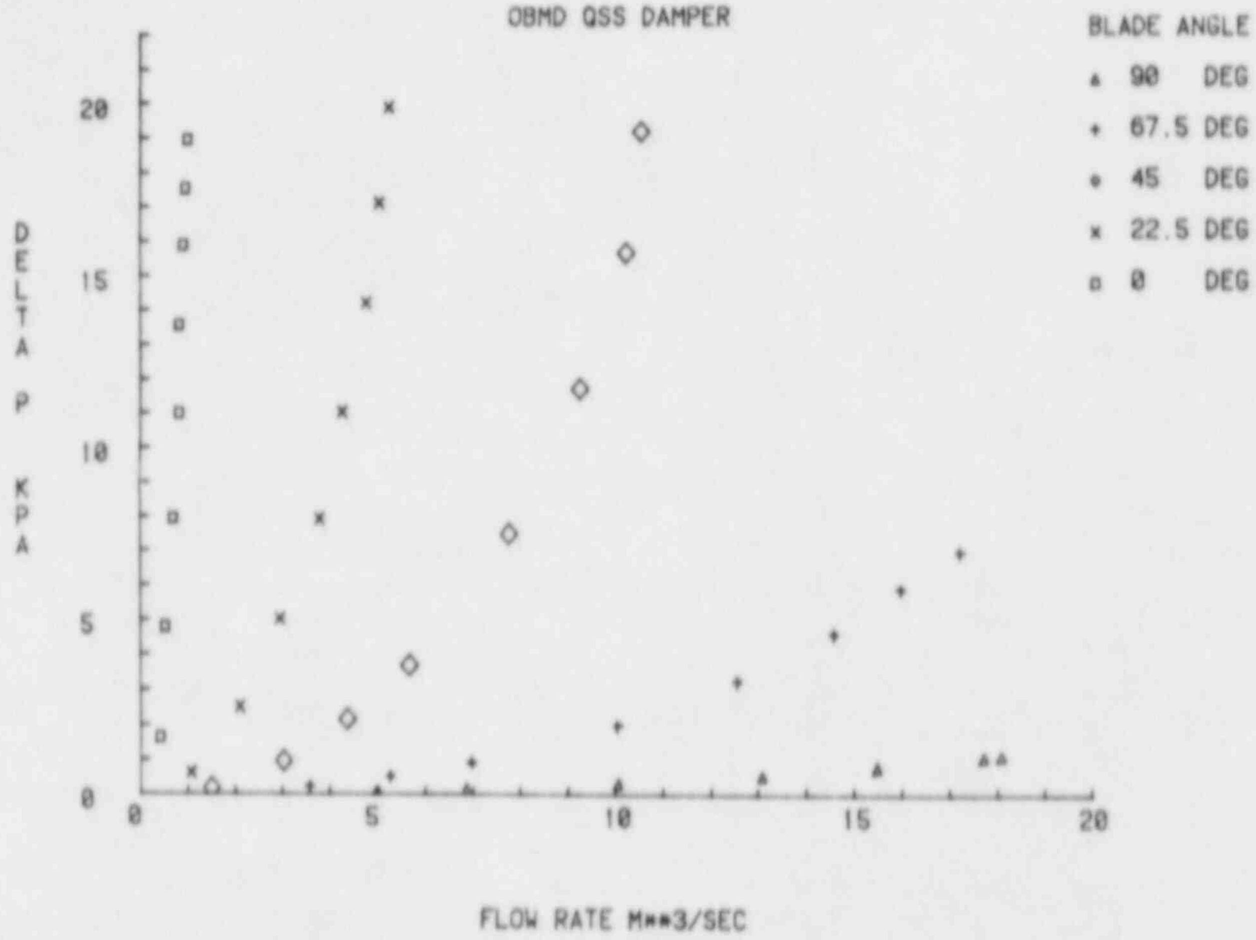

Fig. 12. Opposed-blade, medium-duty damper, quasi-steady state.

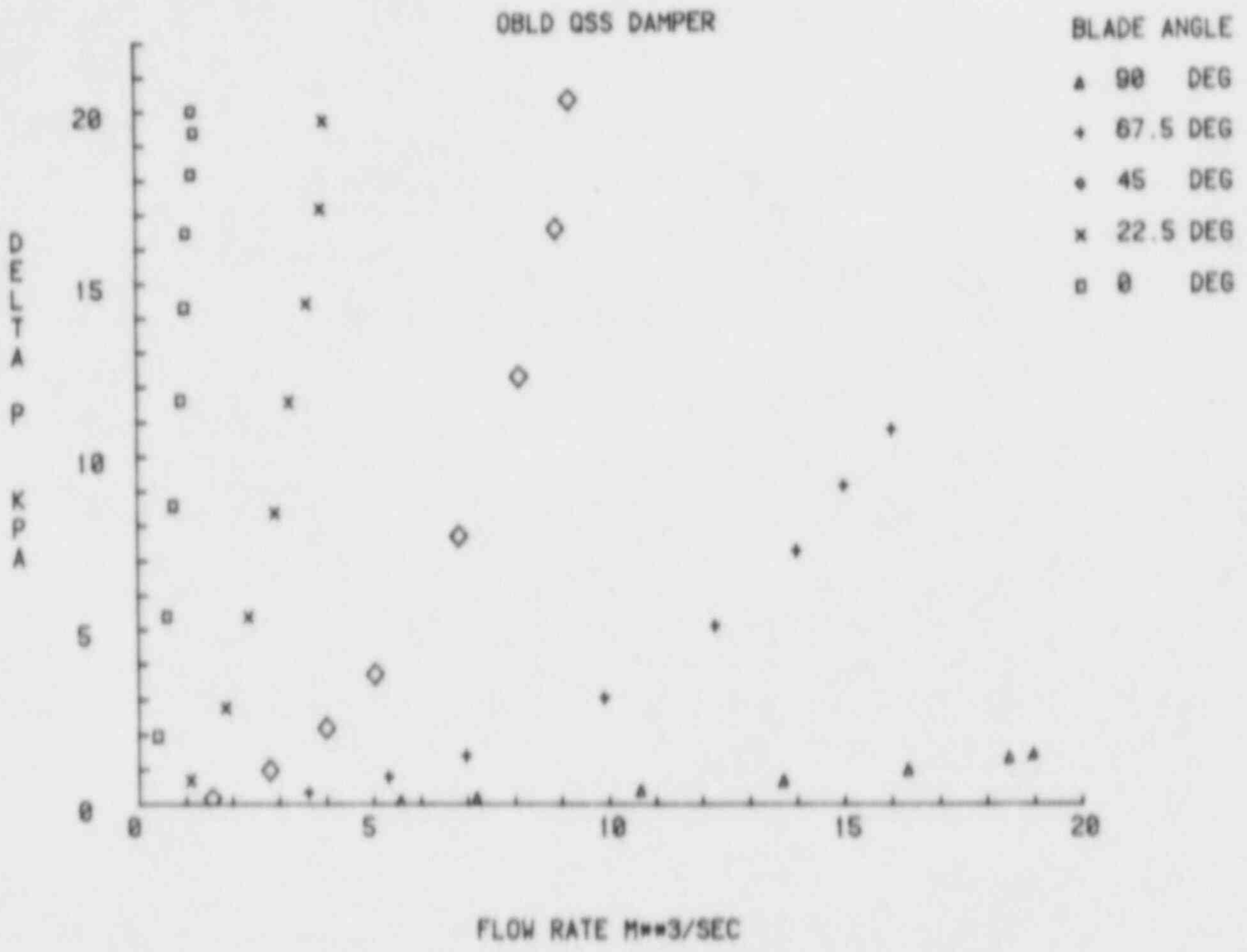

Fig. 13. Opposed-blade, light-duty damper, quasi-steady state.

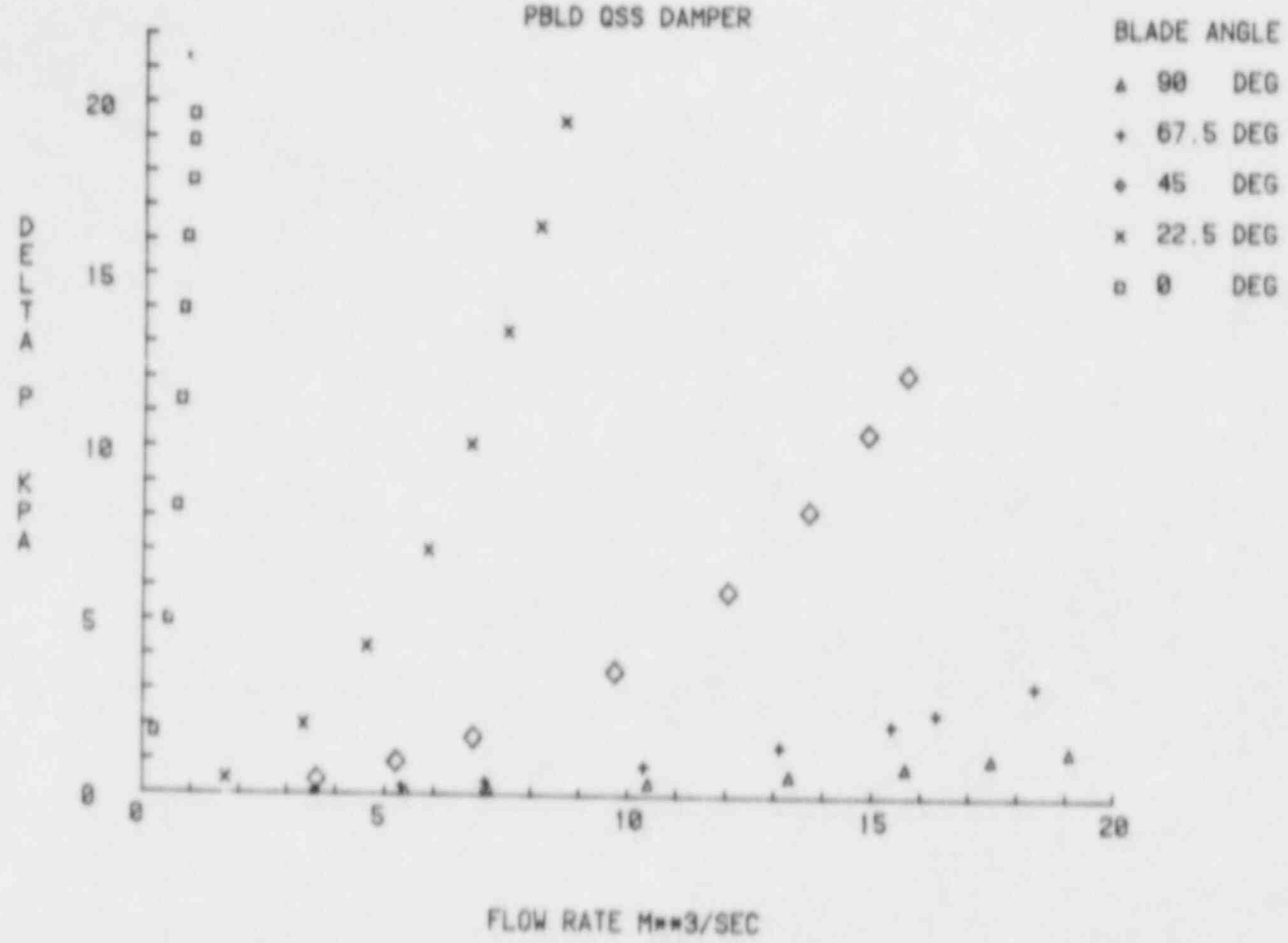

Fig. 14. Parallel-blade, light-duty damper, quasi-steady state.

fully closed position (that is, a blade angle of 0°), the curve of pressure drop as a function of flow rate also is virtually identical for all three types of dampers. In the closed position, the dampers offer maximum resistance to flow, and pressure drop increases very rapidly with flow rate.

The opposed-blade, medium-duty dampers and the opposed-blade, light-duty dampers were nearly identical in configuration except for the gauge of the metal used in their construction. However, the light-duty version offered more resistance to the flow than did the medium-duty version at the same flow rate for blade angles of 22.5°, 45°, and 67.5°. One apparent reason for this difference is the tendency for the blades of the light-duty version to twist toward closure when subjected to high airflow rates. Hence, their effective angle of attack was higher than the blades of the medium-duty damper for the same indicated blade angle. Another reason may be the presence of ribs on the blades of the light-duty damper, which apparently are needed to give the blades rigidity but add to their drag. At all blade angles other than fully open or fully closed, the parallel-blade, light-duty damper created less pressure drop then did the opposed-blade dampers (medium or light duty) at the same flow rate.

The data in Figs. 12--14 can be presented in the following form for ease of use in a ventilation system simulation code such as EVENT or TVENT.

$$Q = P_i(\Delta P)^{0.5} \quad , \tag{14}$$

where P_i is a resistance coefficient, Q is the flow rate, and ΔP is the pressure drop across the dampers. P_i, tabulated in Table II, was determined by a least-squares fit to the data in Figs. 12--14. The details of the least-squares fit and the goodness of fit are discussed in the appendix.

The data in Table II were analyzed further and incorporated into Eq. (14) to yield a relationship for P_i as a function of blade angle, θ. The Table II data are plotted in Figs. 15--17. In addition, a least-squares polynomial fit was made to these data. The resulting equations are quartics of the following general form:

$$P_i = a + b\theta + c\theta^2 + d\theta^3 + e\theta^4 \quad . \tag{15}$$

TABLE II

RESISTANCE COEFFICIENTS FOR OPPOSED-BLADE, MEDIUM-DUTY (OBMD); OPPOSED-BLADE LIGHT-DUTY (OBLD); AND PARALLEL-BLADE, LIGHT-DUTY (PBLD) DAMPERS

Damper	Blade Angle	P_i
OBMD	0.0°	0.237
	22.5°	1.254
	45.0°	2.632
	67.5°	6.739
	90.0°	17.359
OBLD	0.0°	0.273
	22.5°	0.967
	45.0°	2.267
	67.5°	5.168
	90.0°	16.166
PBLD	0.0°	0.226
	22.5°	2.074
	45.0°	4.758
	67.5°	10.584
	90.0°	16.698

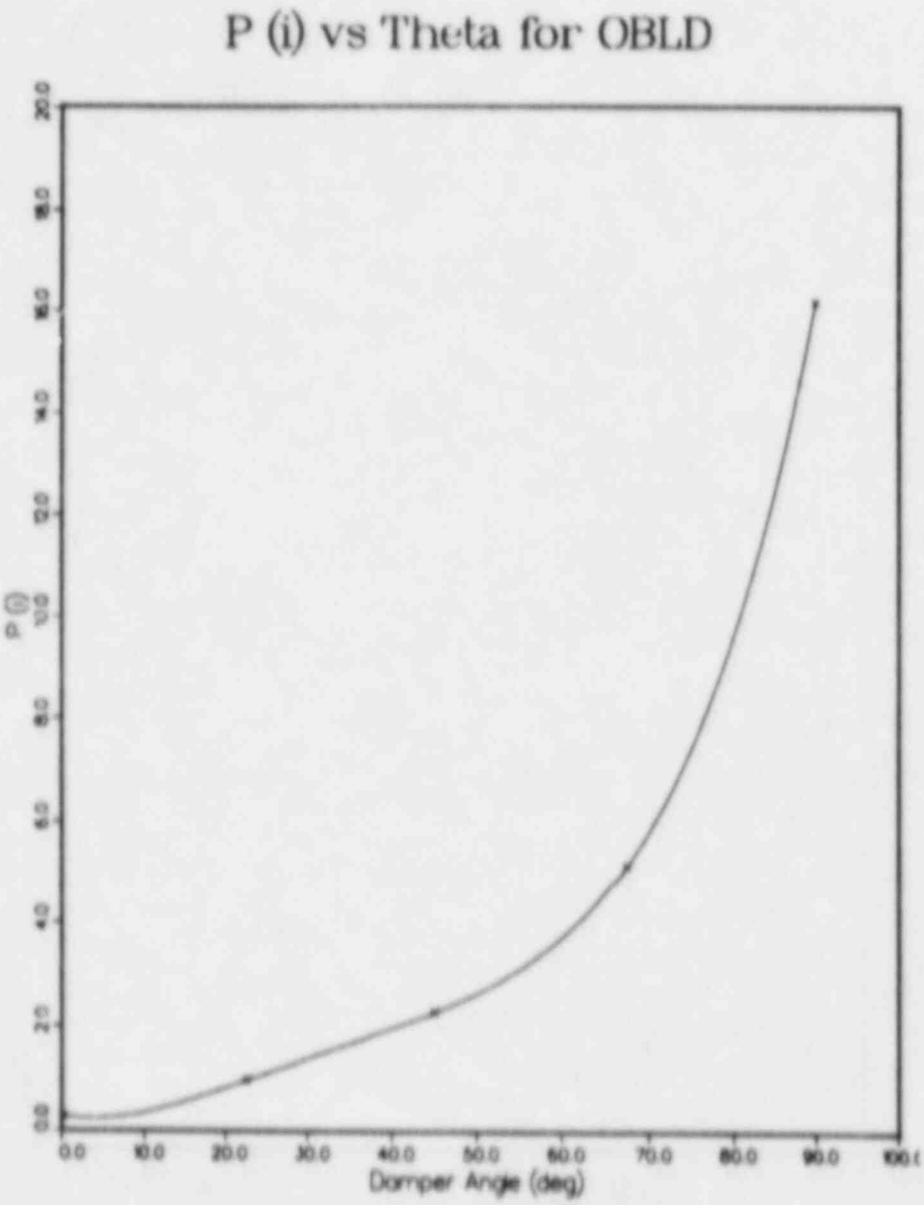

Fig. 15. Pressure drop vs blade angle for OBLD damper.

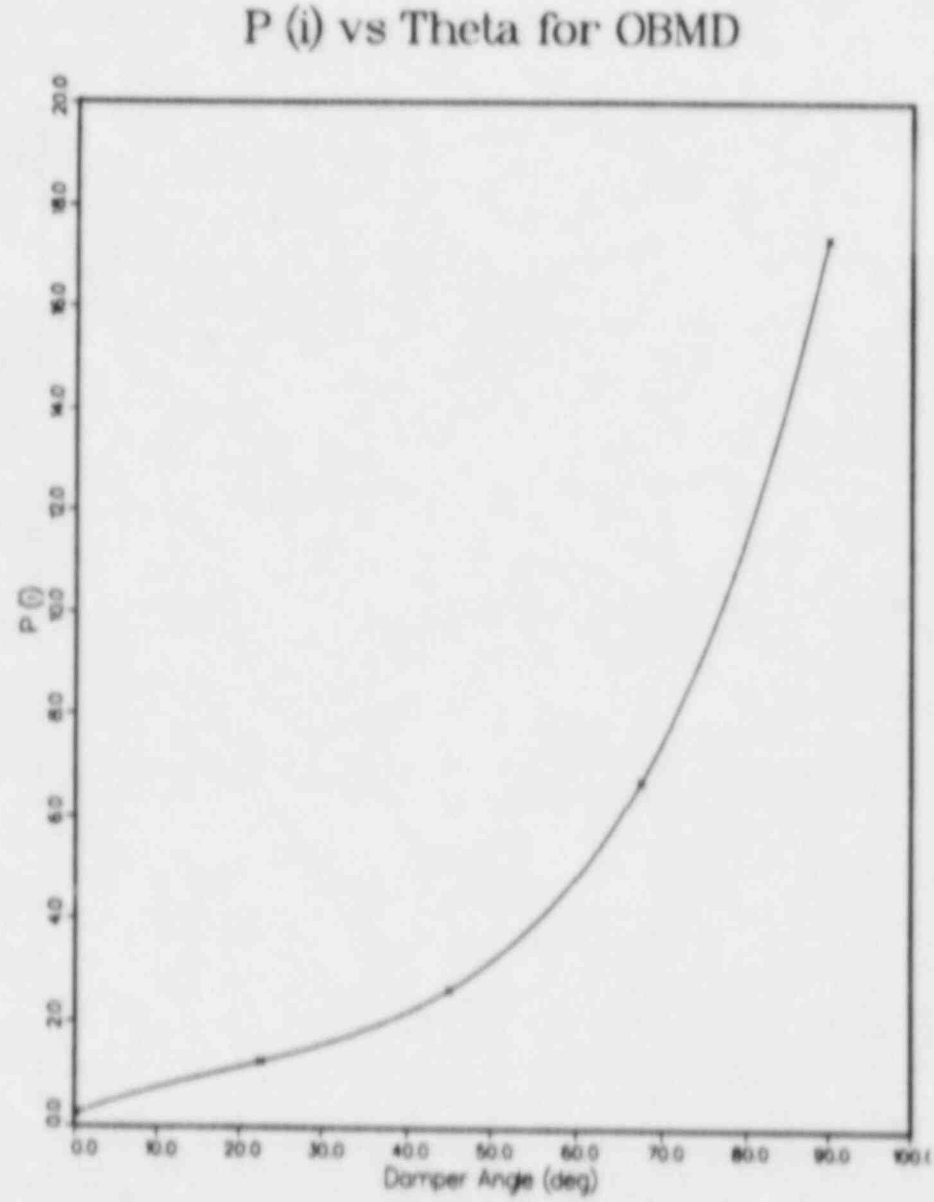

Fig. 16. Pressure drop vs blade angle for OBMD damper.

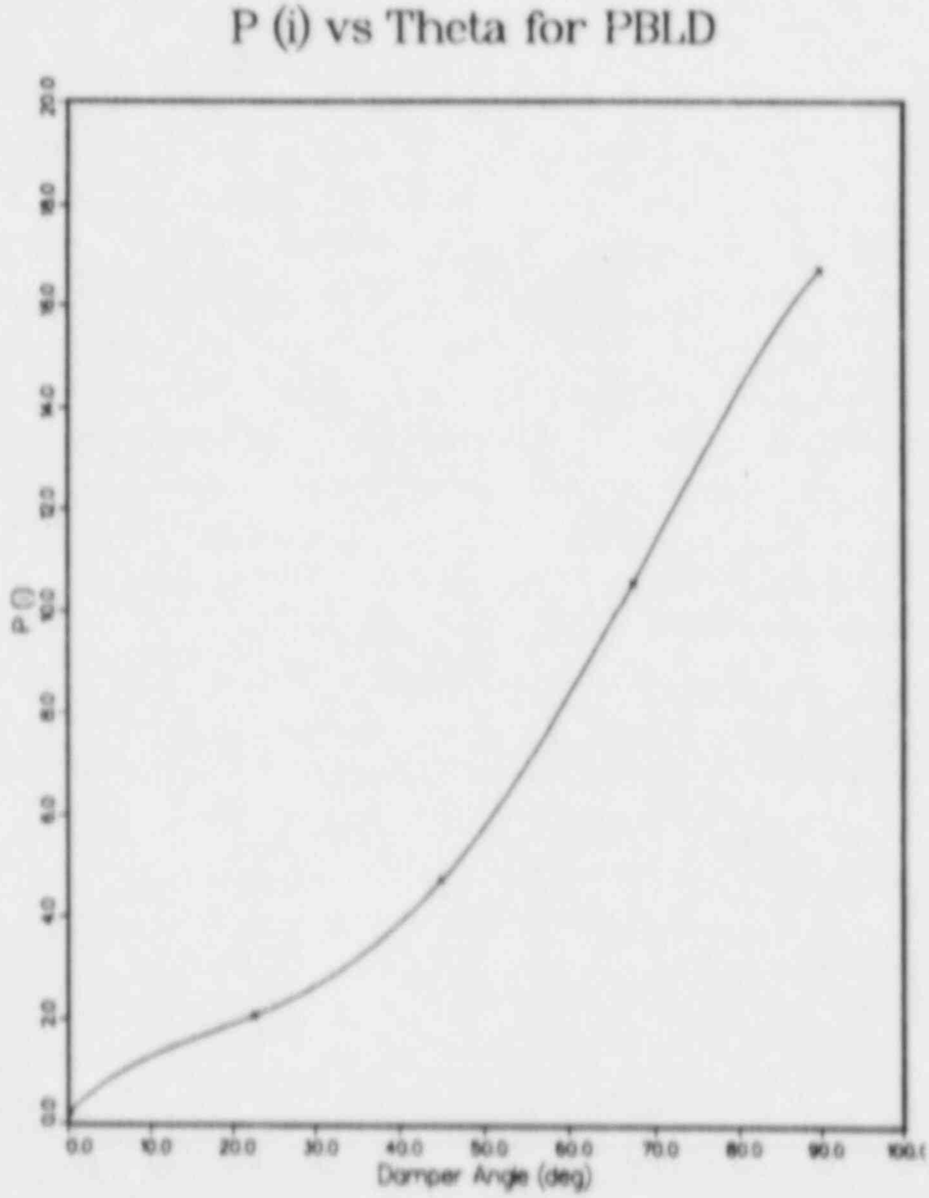

Fig. 17. Pressure drop vs blade angle for PBCD damper.

The coefficients in Eq. (15) are listed in Table III. The fitted curves are shown in Fig. 2.

B. Transient Tests

Figures 18 and 19 show the flow rate and pressure drop as a function of time for a typical transient test (BD 100) of the backdraft damper. The solenoid valves supplying the high-pressure air to the prefilter chamber began opening at time $t = 0$ s. They opened sequentially in such a way that all 12 were open at 1.0 s and remained open for 3.0 s thereafter. The valves began closing at time $t = 4.0$ s; by time $t = 6$ s, all 12 were closed and the flow stopped. Because of the compressibility of the flow and the capacitance of the prefilter chamber, the flow rate did not begin to increase at location PL-3 until about time $t = 0.28$ s. As the velocity continued to increase, the damper began to close at time $t = 0.31$ s (as shown in Table III) and was closed completely at about time $t = 0.91$ s, at which time the flow rate dropped dramatically. The pressure drop across the damper climbed to a maximum value of 20 kPa (3 psi) at time $t = 2.2$ s, where it remained essentially constant until time $t = 4.0$ s. The leakage flow rate for the fully closed damper at a pressure drop of 20 kPa (3 psi) appeared to average about 0.10 m^3/s.

Table IV, which presents the blade angles as a function of time for three backdraft transient tests (BD 98, BD 99, and BD 100), shows that, once this damper is set in motion, closure time ranges from 0.8 s to 1.8 s. Because this is a fairly short time, the event could be modeled by assuming that the damper immediately closes when the local flow rate exceeds the design flow rate at the damper by a specified amount, such as 5%. The leakage flow rate for the fully closed damper would be assumed to be related to pressure drop according to Eq. (14). Then,

TABLE III

COEFFICIENTS FOR EQ. (15)

Damper	a	b	c	d	e
OBMD	2.371×10^{-1}	5.642×10^{-2}	-6.941×10^{-4}	3.460×10^{-6}	2.308×10^{-7}
OBLD	2.732×10^{-1}	-2.943×10^{-2}	4.622×10^{-3}	-1.066×10^{-4}	8.969×10^{-7}
PBLD	2.237×10^{-1}	1.556×10^{-1}	-6.154×10^{-3}	1.475×10^{-4}	-8.419×10^{-7}

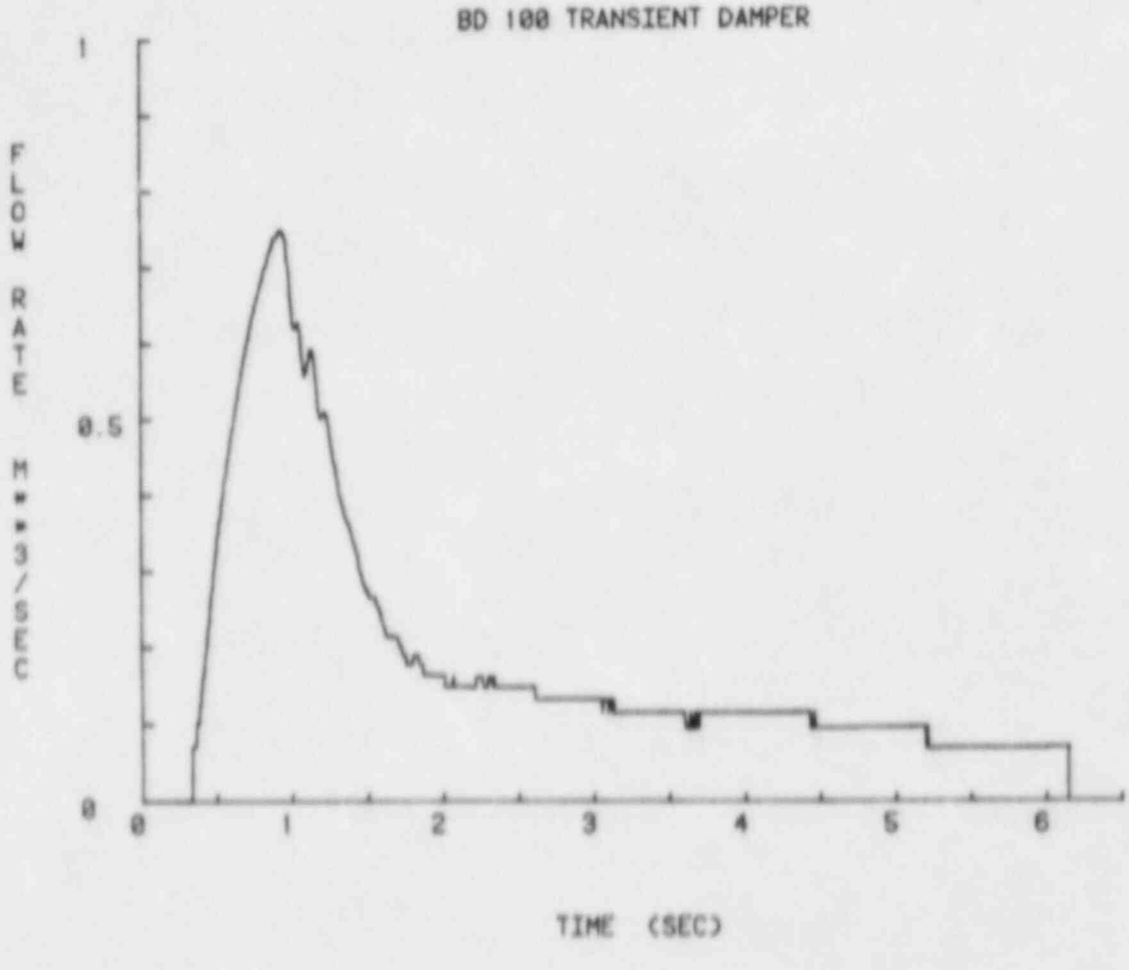

Fig. 18. Backdraft damper, transient test, flow rate vs time.

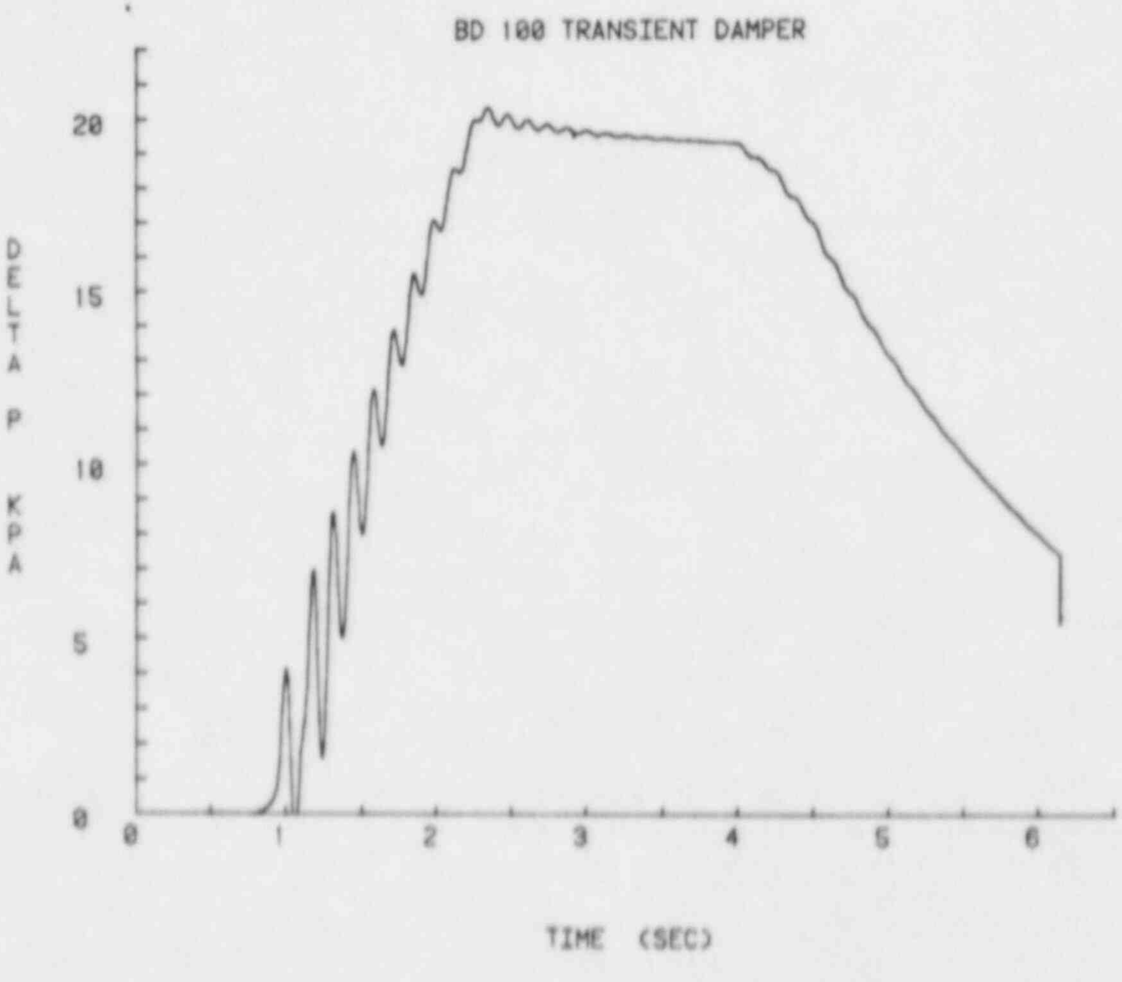

Fig. 19. Backdraft damper, transient test, ΔP vs time.

TABLE IV

BLADE ANGLE AS A FUNCTION OF TIME FOR THREE BACKDRAFT DAMPER TESTS

	Time (s)		
Blade Angle (°)	BD 98	BD 99	BD 100
84	0.88	0.4	.31
63	1.40	0.71	.63
42	1.59	0.83	.71
21	1.69	0.91	.76
0(closed)	1.79	0.98	.80

$$0.1 = P_i(20)^{0.5} \quad ,$$

or

$$P_i = 0.1/(20)^{0.5} = 0.0224 \quad .$$

Thus, for use in a ventilation system simulation code like EVENT or TVENT, the relation between flow rate and pressure drop for a closed backdraft damper could be assumed to be

$$Q = 0.0224(\Delta P)^{0.5} \quad .$$

Figures 20 and 21 present the flow rate and the static pressure rise through the damper as functions of time and for one test of the tornado damper. These figures were plotted from the digital computer data taken during a typical transient test. The valves supplying the prefilter chamber began

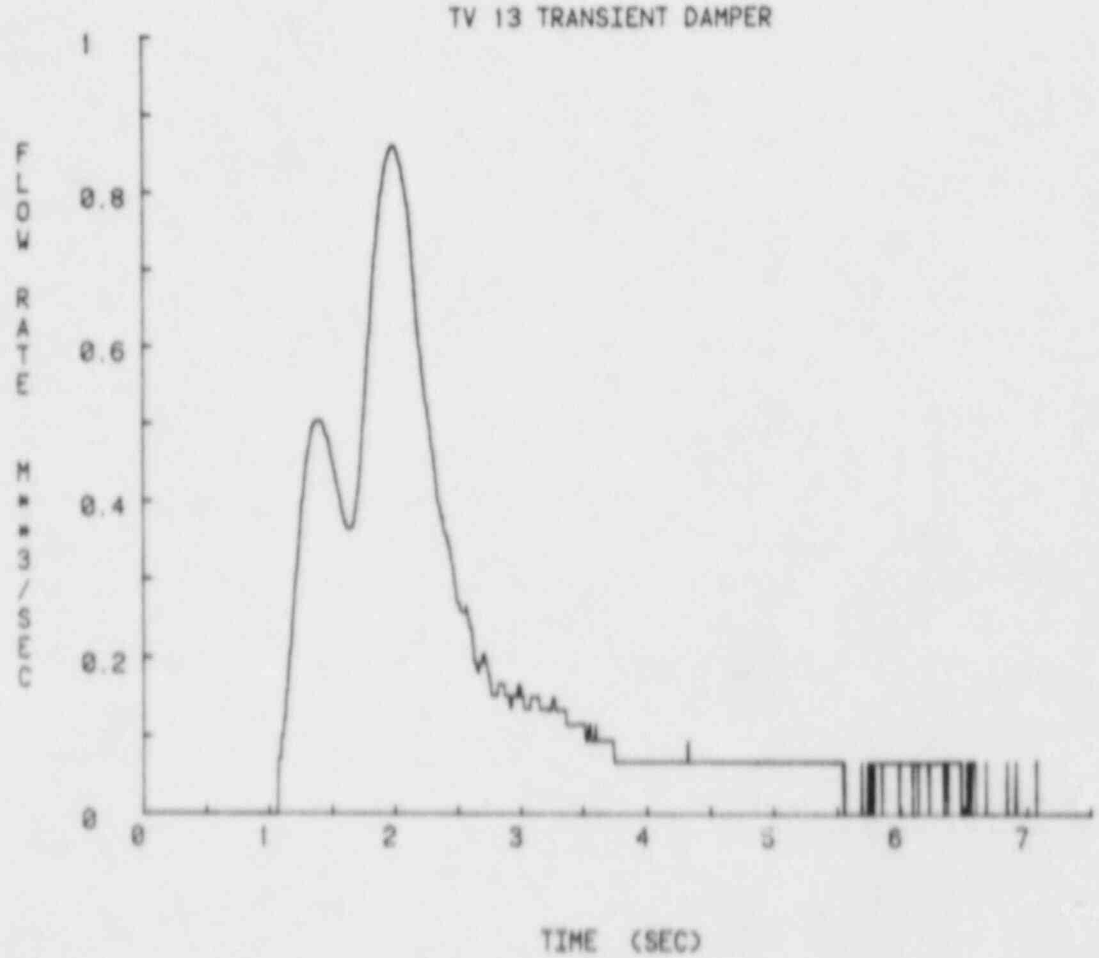

Fig. 20. Techno tornado damper, transient test, flow rate vs time.

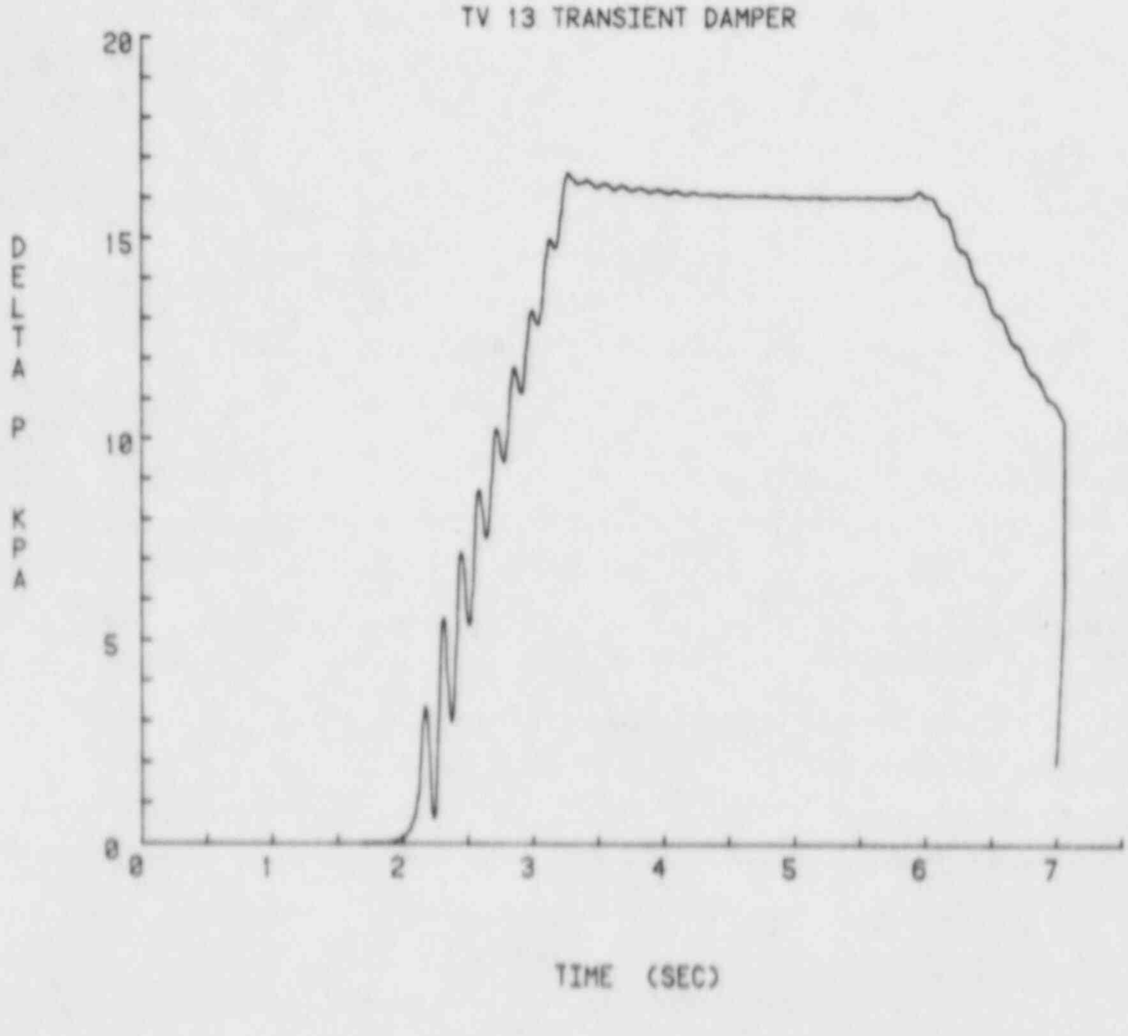

Fig. 21. Techno tornado damper, transient test, ΔP vs time.

opening at time t = 0 s, and all 12 valves were fully open at time t = 1.5 s and remained so until time t = 4.5 s, when they began closing. All 12 were closed by time t = 6 s. Because of the compressibility of the air and the capacitance of the prefilter chamber, the flow rate does not begin to increase at location PL-3 until time t = 1 s. As the velocity increases, the valve begins to close at ~1.42 s, which causes the pressure to begin rising across the damper. Table V shows the blade angle as a function of time for this test. At a time of 1.74 s, the blades were fully closed but then began to bounce about 1° at a frequency of 100 Hz. After about three cycles, the blades bounced open to ~5° at a time of 1.8 s. The flow rate reaches its maximum value at about this time because all 12 supply valves are still fully open. At a time of 1.84 s the blades again are closed and the flow rate drops off rapidly, but the pressure drop across the valve remains constant at ~16 kPa (2.3 psi). The leakage flow rate at full closure and 16 kPa is ~0.08 m^3/s.

C. Special Problems

Two noteworthy structural problems arose during the testing of the dampers. The first was the flexibility of the control linkage of the opposed-blade and parallel-blade dampers, especially the light-duty versions. Although clamped in a set position to keep the blades at a fixed angle, the linkages would flex and cause the effective blade angle to change. When this problem was recognized, the linkages were strengthened by adding more clamps. In this way, most of the blade movement during quasi-steady testing was eliminated and probably was not important except for the light-duty versions of the dampers.

The second structural problem occurred for the backdraft damper. The blades of the damper are made of sheet metal folded around a shaft about which they pivot. The sheet metal is spot-welded to the shafts in about four places. Transient testing of the backdraft damper caused these spot welds to fail randomly and allowed the blades to twist relative to the shafts. This would occur differently for each test, causing a great variance in the test results. The problem was solved by adding more welds to the blades. The data obtained for transient testing of the backdraft damper after the blade/shaft connection was strengthened proved to be repeatable and consistent; they are the data presented in this report.

TABLE V

BLADE ANGLE AS FUNCTION OF TIME
FOR TORNADO DAMPER
TEST NO. 13

Time s	Valve Position (°)
1.42	55
1.56	44
1.63	33
1.68	22
1.71	11
1.74	0
1.75	1
1.76	0
1.77	1
1.78	0
1.80	5
1.84	0

V. SUMMARY AND CONCLUSIONS

The quasi-steady testing of the opposed-blade and parallel-blade dampers provided information about the relationship between the pressure drop through the dampers and the flow rate for fixed blade angles. This relationship was approximated by a formula that can be used in a computer simulation of flow and pressure drop through a nuclear facility ventilation system. Further, this relationsnip was extended to relate the damper resistance coefficient as a function of blade angle. If this relationship is coupled with the control system that maintains pressure or flow control for the ventilation system, the dynamic response of the control system can be included in the analysis. For example, if a pressure point is controlled within the system, the damper blade angle can

be adjusted to respond to the pressure change as the pressure varies. This would require a control system module to be added to computer simulation codes such as TVENT.

Transient testing of a backdraft damper proved that it closed within a range of 0.8 to 1.8 s. The assumption that the leakage flow rate for the fully closed backdraft damper can be related to the pressure drop through the damper by a formula similar to that developed for the opposed-blade and parallel-blade dampers appears valid. The backdraft damper has a serious structural problem for pressure pulses equivalent to the NRC Region I standard tornado pulse. The welds that hold the sheet metal blades to the shaft on which they pivot break, rendering the damper ineffective. When subjected to a tornado-like pressure pulse, the tornado damper closes in ~1.84 s after bouncing several times. Closure time for this damper could be reduced to 1.74 s if the bounce could be eliminated. A summary of the formulas that can be used for damper simulation in computer codes like TVENT and EVENT are given in Table VI.

TABLE VI

DAMPER SIMULATION FORMULAS

Damper	Formula
OBMD	$Q = P_i\ (\Delta P)^{0.5}$
	or
OBLD, PBLD	$Q = (a + b\theta + c\theta^2 + d\theta^3 + e\theta^4)\ (\Delta P)^{0.5}$
Backdraft	$Q = 0.0224\ (\Delta P)^{0.5}$ at closure[a]

[a]If local flow rate increases by 5 .

REFERENCES

1. K. H. Duerre, R. W. Andrae, and W. S. Gregory, "TVENT-A Computer Program for Analysis of Tornado-Induced Transients in Ventilation Systems," Los Alamos Scientific Laboratory report LA-7397-M (July 1978).

2. "Test Methods for Louvers, Dampers and Shutters," AMCA 500-75 (Air Movement and Control Association, Inc., Arlington Heights, Illinois, October 18, 1973).

3. "Laboratory Methods of Testing Fans for Rating," AMCA 210-74 (Air Movement and Control Association, Inc., Arlington Heights, Illinois, 1967).

APPENDIX

TABULAR QUASI-STEADY-STATE DATA AND A LEAST-SQUARES FIT TO RELATE FLOW RATE TO PRESSURE DROP

A Hewlett-Packard-supplied least-squares subroutine called FITTER was used on an HP-9845B digital computer to fit the quasi-steady-state data taken for the opposed-blade, medium-duty; the opposed-blade, light-duty; and the parallel-blade, light-duty dampers to the equation

$$Q = P_i(\Delta P)^{0.5} \quad ,$$

in which P_i is a resistance coefficient to be determined, Q is the flow rate, and ΔP is the pressure drop across the dampers. The values of P_i were presented in Table II.

The following tables and figures show the actual computer output of the curve fits and represent (1) the experimental data, (2) the value of P_i, (3) the fitting error, and (4) a plot in which the solid line is curve-fit to the experimental data points (stars) as a graphic demonstration of the goodness of fit. Pressure drop is given in kilopascals, and flow rate is given in cubic meters per second throughout.

OBMD 90 DEGREES CURVE FIT

Created on 07-05-83

OBSERVATION	DEL P (kPa)	FLOW RATE
1	0.073	4.981
2	0.145	6.862
3	0.313	10.065
4	0.533	13.077
5	0.788	15.475
6	1.084	17.715
7	1.125	18.079

FINAL RESULT OF CURVE FIT

Dataset title: OBMD 90 DEGREES CURVE FIT

Model used:

User Defined Eq.

The estimated parameter values after three iterations are

P(1) = 17.359 .

FITTING ERROR (in Y-axis units)

Maximum error between any data point and the curve is 0.4037410835.

Overall standard error in estimate is 0.33651794881.

OBMD 67.5 DEGREES CURVE FIT

Created on 07-05-83

OBSERVATION	DEL P (kPa)	FLOW RATE
1	0.237	3.568
2	0.532	5.256
3	0.924	6.967
4	1.993	10.038
5	3.263	12.548
6	4.614	14.572
7	5.9	15.981
8	6.982	17.222

FINAL RESULT OF CURVE FIT

Dataset title: OBMD 67.5 DEGREES CURVE FIT

Model used:

User Defined Eq.

The estimated parameter values after three iterations are

P(1) = 6.7388.

FITTING ERROR (in Y-axis units)

Maximum error between any data point and the curve is 0.5842509364.

Overall standard error in estimate is 0.439974316404.

OBMD 45 DEGREES CURVE FIT

Created on 07-05-83

OBSERVATION	DEL P (kPa)	FLOW RATE
1	0.186	1.511
2	0.973	3.021
3	2.17	4.372
4	3.707	5.663
5	7.519	7.767
6	11.743	9.286
7	15.671	10.253
8	19.174	10.568

FINAL RESULT OF CURVE FIT

Dataset title: OBMD 45 DEGREES CURVE FIT

Model used:

User Defined Eq.

The estimated parameter values after three iterations are

P(1) = 2.6325.

FITTING ERROR (in Y-axis units)

Maximum error between any data point and the curve is 0.9592252334.

Overall standard error in estimate is 0.565444785155.

OBMD 22.5 DEGREES CURVE FIT

Created on 07-05-83

OBSERVATION	DEL P (kPa)	FLOW RATE
1	0.621	1.083
2	2.516	2.112
3	5.024	2.963
4	7.924	3.798
5	11.051	4.288
6	14.224	4.782
7	17.108	5.08
8	19.891	5.269

FINAL RESULT OF CURVE FIT

Dataset title: OBMD 22.5 DEGREES CURVE FIT
Model used:
User Defined Eq.

The estimated parameter values after three iterations are

P(1) = 1.2544.

FITTING ERROR (in Y-axis units)

Maximum error between any data point and the curve is 0.32553962243.
Overall standard error in estimate is 0.190698964244.

OBMD 0 DEGREES CURVE FIT

Created on 07-05-83

OBSERVATION	DEL P (kPa)	FLOW RATE
1	1.632	0.415
2	4.784	0.528
3	7.935	0.701
4	10.999	0.831
5	13.556	0.828
6	15.886	0.927
7	17.533	0.971
8	19.948	1.014

FINAL RESULT OF CURVE FIT

Dataset title: OBMD 0 DEGREES CURVE FIT

Model used:

User Defined Eq.

The estimated parameter values after three iterations are

P(1) = 0.23708.

FITTING ERROR (in Y-axis units)

Maximum error between any data point and the curve is 0.11213087995.

Overall standard error in estimate is 5.19554392857E-02.

OBLD 90 DEGREES CURVE FIT

Created on 07-05-83

OBSERVATION	DEL P (kPa)	FLOW RATE
1	0.097	5.562
2	0.179	7.175
3	0.406	10.664
4	0.682	13.701
5	1.004	16.335
6	1.347	18.457
7	1.45	18.96

FINAL RESULT OF CURVE FIT

Dataset title: OBLD 90 DEGREES CURVE FIT

Model used:

User Defined Eq.

The estimated parameter values after one iteration are

P(1) = 16.166.

FITTING ERROR (in Y-axis units)

Maximum error between any data point and the curve is 0.52712791288.

Overall standard error in estimate is 0.411030577395.

OBLD 67.5 DEGREES CURVE FIT

Created on 07-05-83

OBSERVATION	DEL P (kPa)	FLOW RATE
1	0.361	3.602
2	0.815	5.31
3	1.418	6.954
4	3.055	9.913
5	5.134	12.288
6	7.291	14.01
7	9.164	15.024
8	10.775	16.503

FINAL RESULT OF CURVE FIT

Dataset title: OBLD 67.5 DEGREES CURVE FIT

Model used:

User Defined Eq.

The estimated parameter values after two iterations are

P(1) = 5.2058.

FITTING ERROR (in Y-axis units)

Maximum error between any data point and the curve is 0.81401212393.

Overall standard error in estimate is 0.649991928908.

OBLD 45 DEGREES CURVE FIT

Created on 07-05-83

OBSERVATION	DEL P (kPa)	FLOW RATE
1	0.173	1.553
2	0.995	2.797
3	2.199	3.996
4	3.746	5.041
5	7.722	6.848
6	12.303	8.171
7	16.569	8.972
8	20.299	9.266

FINAL RESULT OF CURVE FIT

Dataset title: OBLD 45 DEGREES CURVE FIT

Model used:

User Defined Eq.

The estimated parameter values after three iterations are

P(1) = 2.2666.

FITTING ERROR (in Y-axis units)

Maximum error between any data point and the curve is 0.9460329213.

Overall standard error in estimate is 0.632555731789.

OBLD 22.5 DEGREES CURVE FIT

Created on 07-05-83

OBSERVATION	DEL P (kPa)	FLOW RATE
1	0.697	1.102
2	2.77	1.861
3	5.383	2.364
4	8.388	2.939
5	11.573	3.273
6	14.421	3.273
7	17.158	3.97
8	19.722	4.054

FINAL RESULT OF CURVE FIT

Dataset title: OBLD 22.5 DEGREES CURVE FIT

Model used:

User Defined Eq.

The estimated parameter values after three iterations are

P(1) = 0.9672.

FITTING ERROR (in Y-axis units)

Maximum error between any data point and the curve is 0.29451832192.

Overall standard error in estimate is 0.186449855596.

OBLD 0 DEGREES CURVE FIT

Created on 07-05-83

OBSERVATION	DEL P (kPa)	FLOW RATE
1	1.959	4.05
2	5.378	0.617
3	8.596	0.765
4	11.623	0.938
5	14.303	1.029
6	16.467	1.071
7	18.174	1.192
8	19.386	4.206
9	20.013	1.206

FINAL RESULT OF CURVE FIT

Dataset title: OBLD 0 DEGREES CURVE FIT

Model used:

User Defined Eq.

The estimated parameter values after three iterations are

P(1) = 0.27325.

FITTING ERROR (in Y-axis units)

Maximum error between any data point and the curve is 0.04989294134.

Overall standard error in estimate is 2.97456802571E-02.

PBLD 90 DEGREES CURVE FIT

Created on 07-05-83

OBSERVATION	DEL P (kPa)	FLOW RATE
1	0.046	3.591
2	0.099	5.424
3	0.172	7.146
4	0.372	10.428
5	0.611	13.319
6	0.876	15.697
7	1.126	17.481
8	1.343	19.079

FINAL RESULT OF CURVE FIT

Dataset title: PBLD 90 DEGREES CURVE FIT

Model used:

User Defined Eq.

The estimated parameter values after three iterations are

P(1) = 16.698.

FITTING ERROR (in Y-axis units)

Maximum error between any data point and the curve is 0.2719576756.

Overall standard error in estimate is 0.221518908235.

PBLD 67.5 DEGREES CURVE FIT

Created on 07-05-83

OBSERVATION	DEL P (kPa)	FLOW RATE
1	0.107	3.57
2	0.234	5.347
3	0.404	7.061
4	0.864	10.34
5	1.46	13.126
6	2.08	15.413
7	2.433	16.333
8	3.226	18.358

FINAL RESULT OF CURVE FIT

Dataset title: PBLD 67.5 DEGREES CURVE FIT
Model used:
User Defined Eq.

The estimated parameter values after three iterations are

P(1) = 10.584.

FITTING ERROR (in Y-axis units)

Maximum error between any data point and the curve is 0.6519954407.
Overall standard error in estimate is 0.381446799643.

PBLD 45 DEGREES CURVE FIT

Created on 07-05-83

OBSERVATION	DEL P (kPa)	FLOW RATE
1	0.446	3.605
2	0.961	5.229
3	1.669	6.817
4	3.573	9.745
5	5.885	12.053
6	8.222	13.706
7	10.459	14.911
8	12.156	15.725

FINAL RESULT OF CURVE FIT

Dataset title: PBLD 45 DEGREES CURVE FIT

Model used:

User Defined Eq.

The estimated parameter values after three iterations are

P(1) = 4.7578.

FITTING ERROR (in Y-axis units)

Maximum error between any data point and the curve is 0.8632865051.

Overall standard error in estimate is 0.627156174612.

PBLD 22.5 DEGREES CURVE FIT

Created on 07-05-83

OBSERVATION	DEL P (kPa)	FLOW RATE
1	0.459	1.705
2	2.018	3.331
3	4.258	4.627
4	7.041	5.879
5	10.107	6.775
6	13.345	7.528
7	16.4	8.189
8	19.454	8.686

FINAL RESULT OF CURVE FIT

Dataset title: PBLD 22.5 DEGREES CURVE FIT

Model used:

User Defined Eq.

The estimated parameter values after three iterations are

P(1) = 2.0737.

FITTING ERROR (in Y-axis units)

Maximum error between any data point and the curve is 0.46040406351.

Overall standard error in estimate is 0.336429519076.

PBLD 0 DEGREES CURVE FIT

Created on 07-05-83

OBSERVATION	DEL P (kPa)	FLOW RATE
1	1.774	0.234
2	4.981	0.517
3	8.267	0.688
4	11.32	0.75
5	13.964	0.804
6	16.047	0.875
7	17.73	0.977
8	18.882	1.002
9	19.647	1.012

FINAL RESULT OF CURVE FIT

Dataset title: PBLD 0 DEGREES CURVE FIT

Model used:

User Defined Eq.

The estimated parameter values after three iterations are

P(1) = 0.22582.

FITTING ERROR (in Y-axis units)

Maximum error between any data point and the curve is 0.066773251528.

Overall standard error in estimate is 3.5218105544E-02.

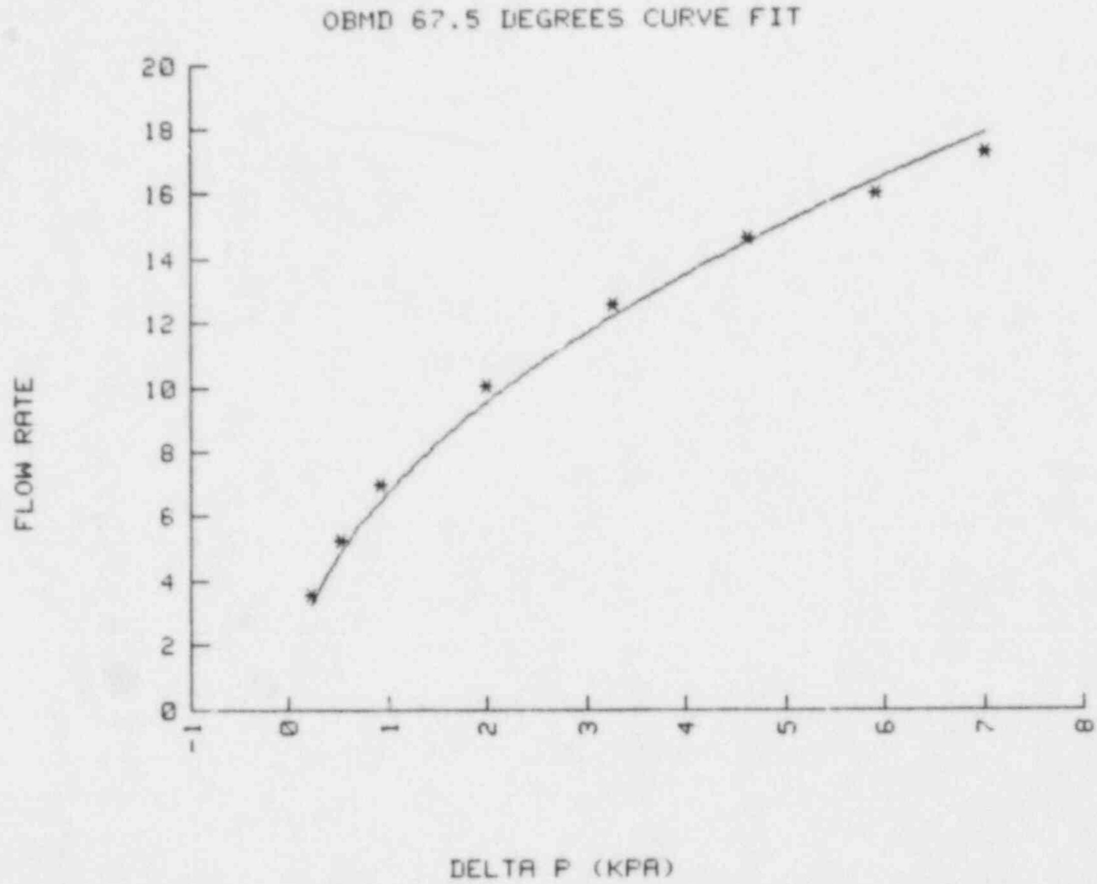
OBMD 67.5 DEGREES CURVE FIT
FLOW RATE
DELTA P (KPA)
20
18
16
14
12
10
8
6
4
2
0
-1
0
1
2
3
4
5
6
7
8

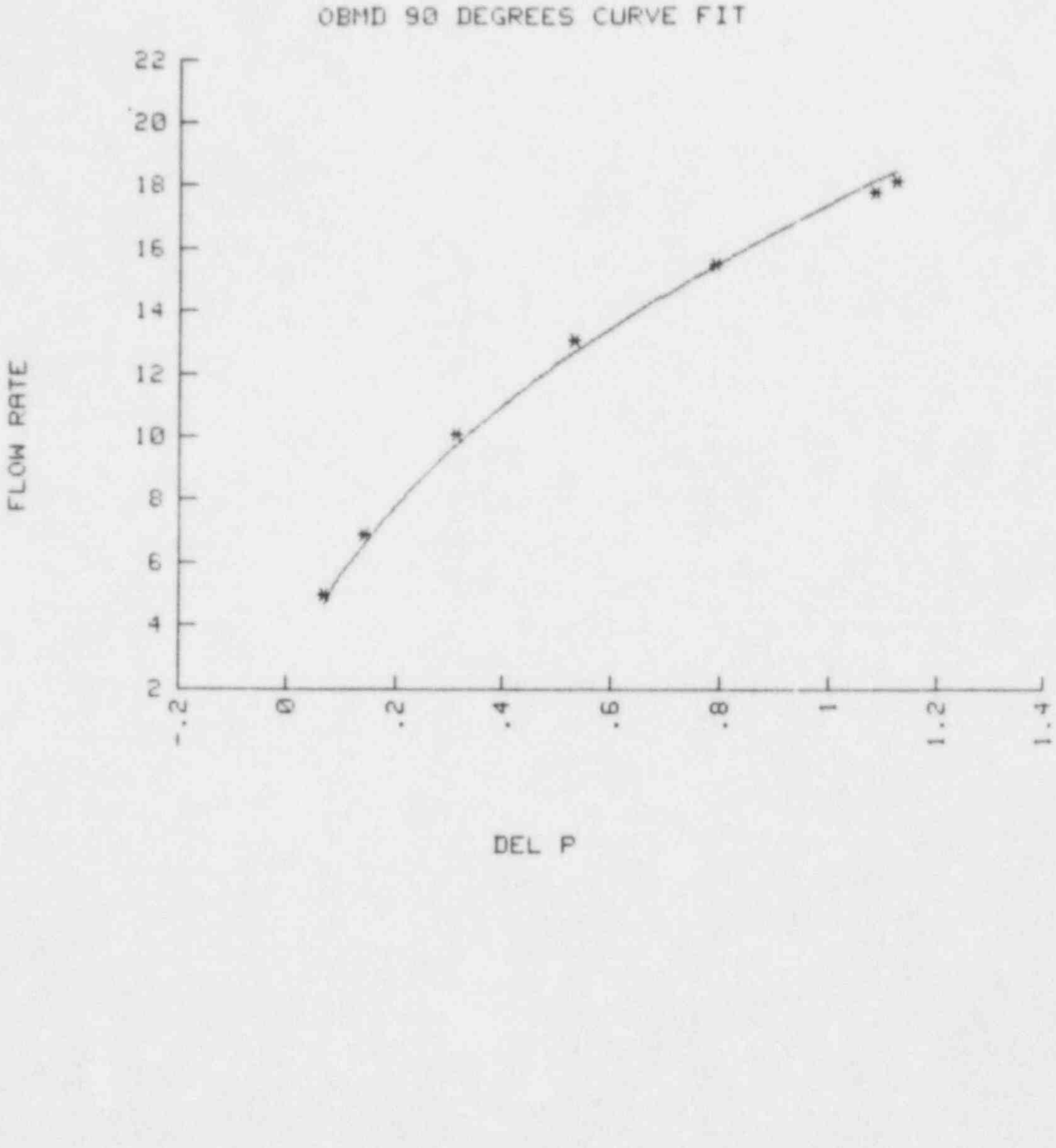
OBMD 90 DEGREES CURVE FIT
FLOW RATE
22
20
18
16
14
12
10
8
6
4
2
-.2
0
.2
.4
.6
.8
1
1.2
1.4
DEL P

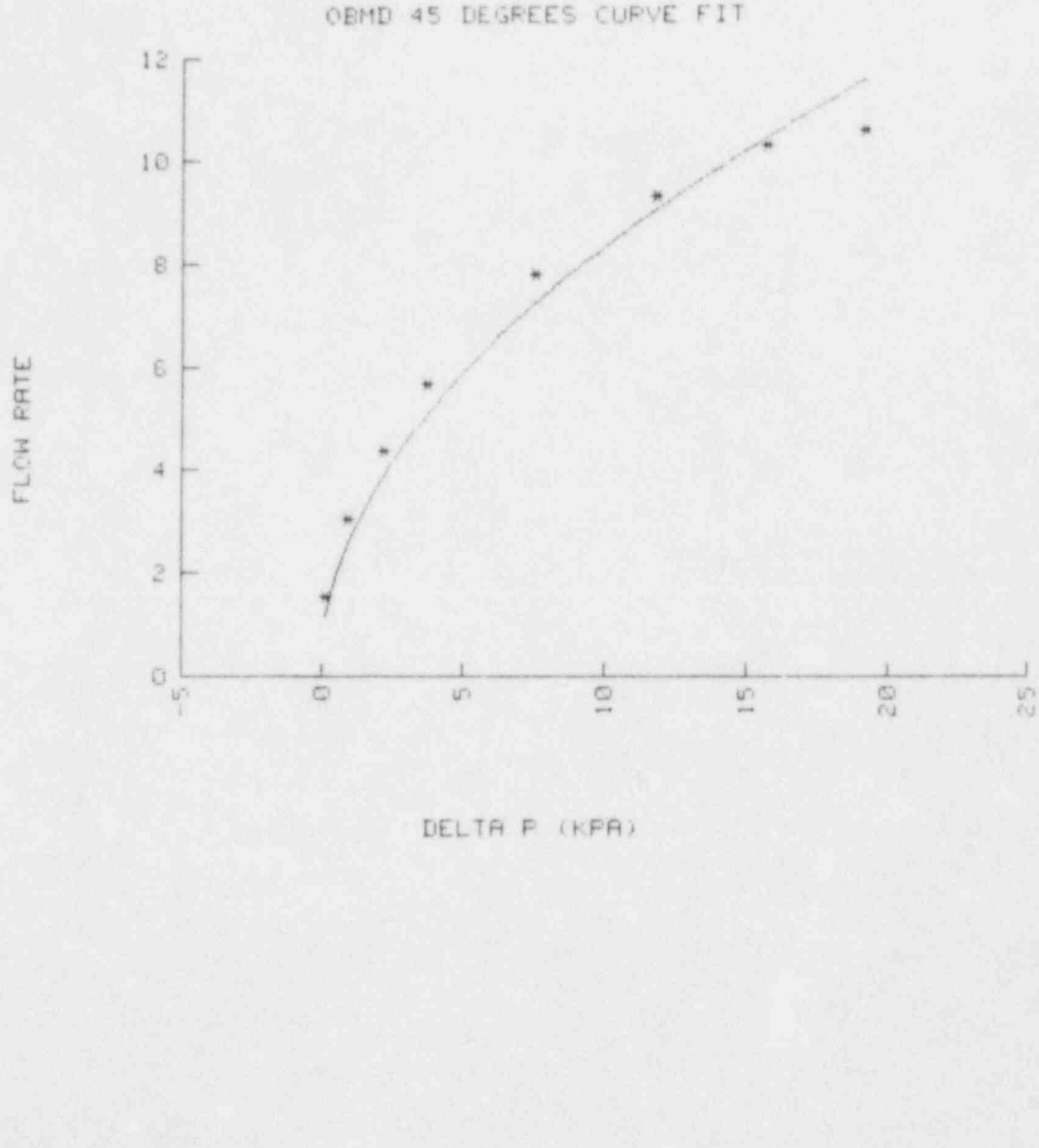
OBMD 45 DEGREES CURVE FIT
FLOW RATE
DELTA P (KPA)
0
2
4
6
8
10
12
-5
0
5
10
15
20
25

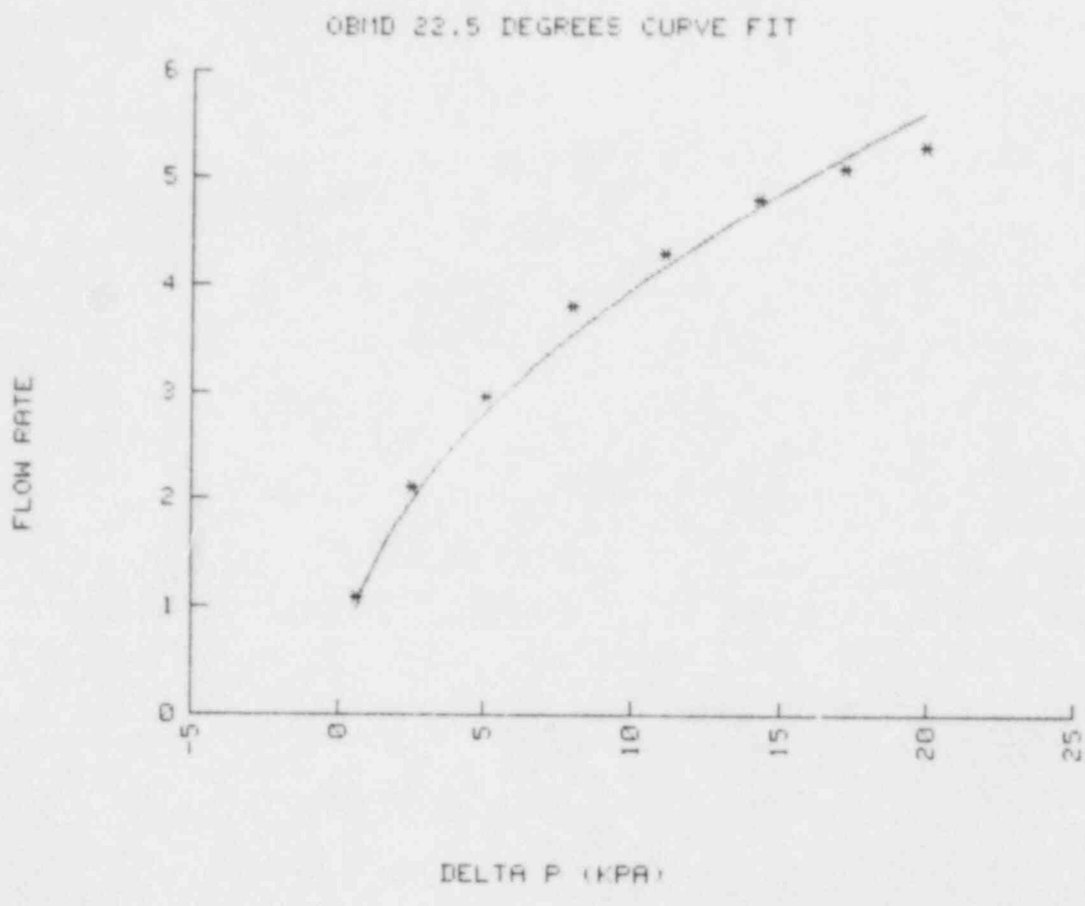

OBMD 22.5 DEGREES CURVE FIT
FLOW RATE
DELTA P (KPA)
0
1
2
3
4
5
6
-5
0
5
10
15
20
25

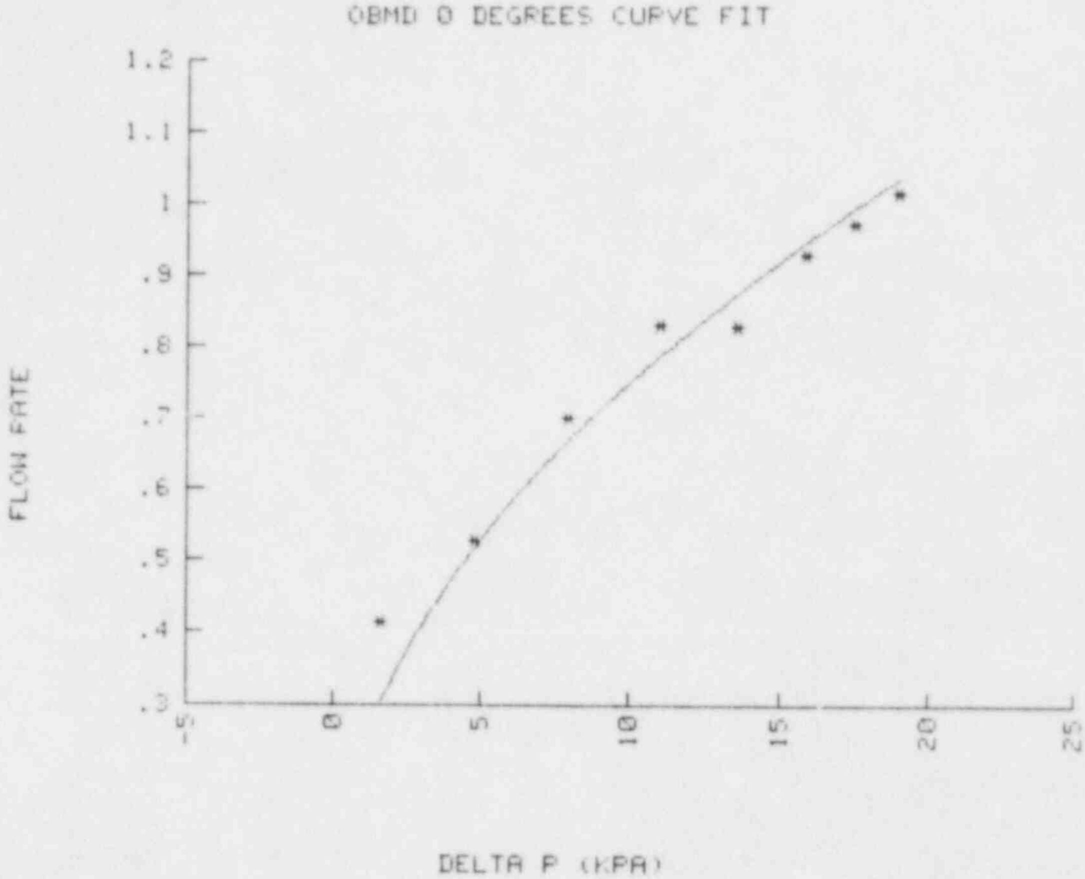

OBMD 0 DEGREES CURVE FIT
1.2
1.1
1
.9
.8
.7
.6
.5
.4
.3
FLOW RATE
-5
0
5
10
15
20
25
DELTA P (KPA)

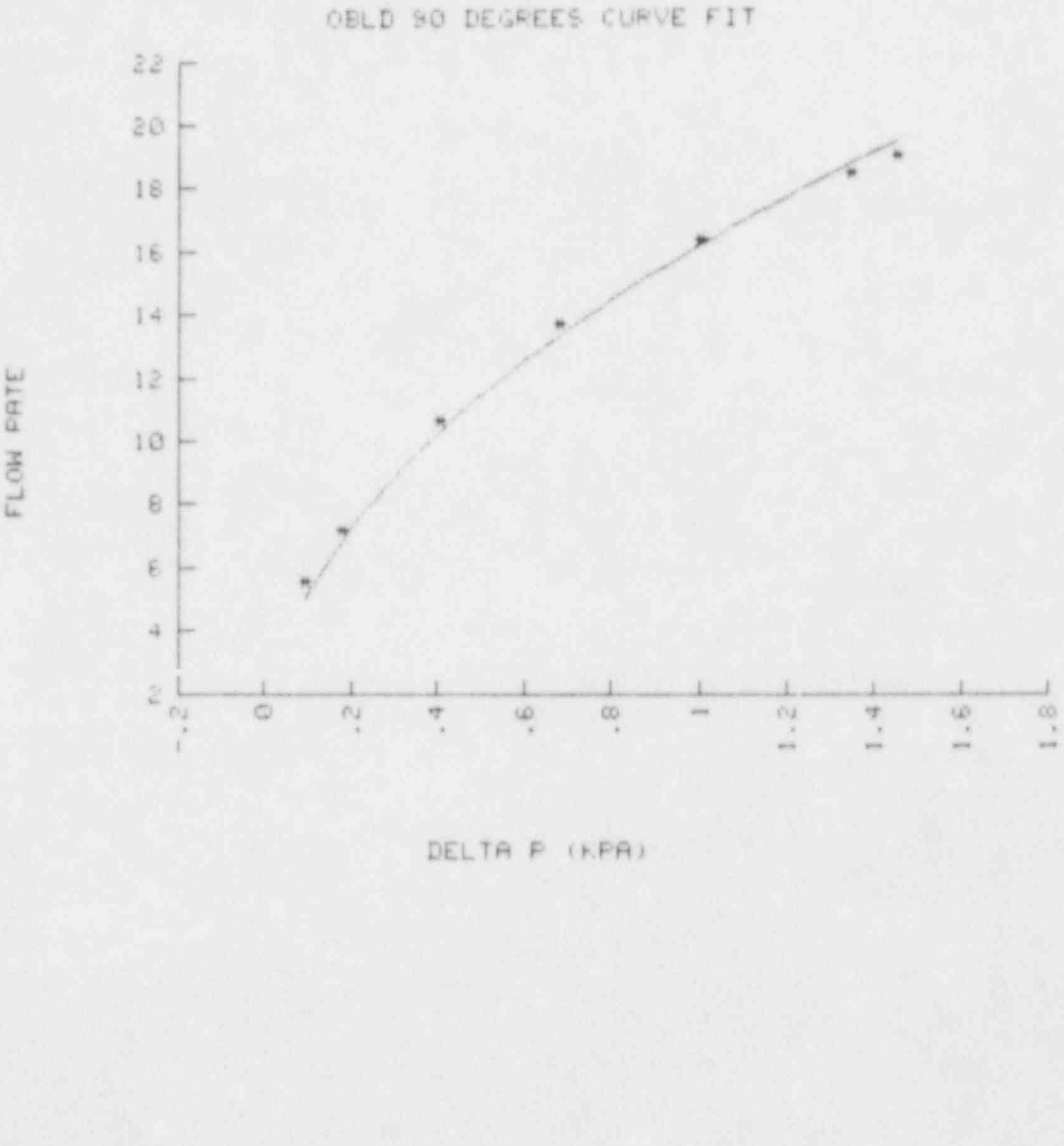
OBLD 90 DEGREES CURVE FIT
FLOW RATE
DELTA P (KPA)
22
20
18
16
14
12
10
8
6
4
2
-.2
0
.2
.4
.6
.8
1
1.2
1.4
1.6
1.8

OBLD 67.5 DEGREES CURVE FIT

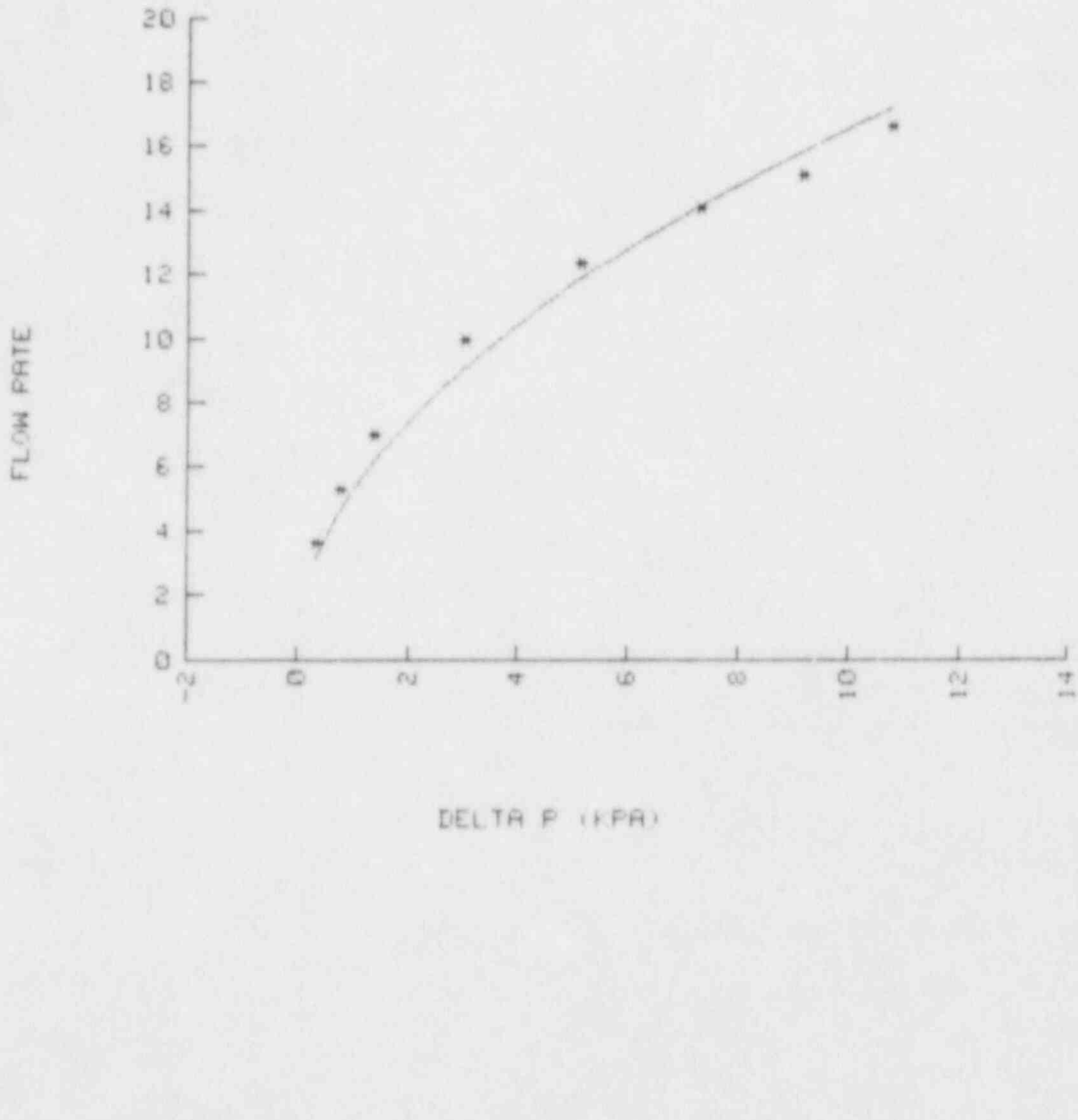

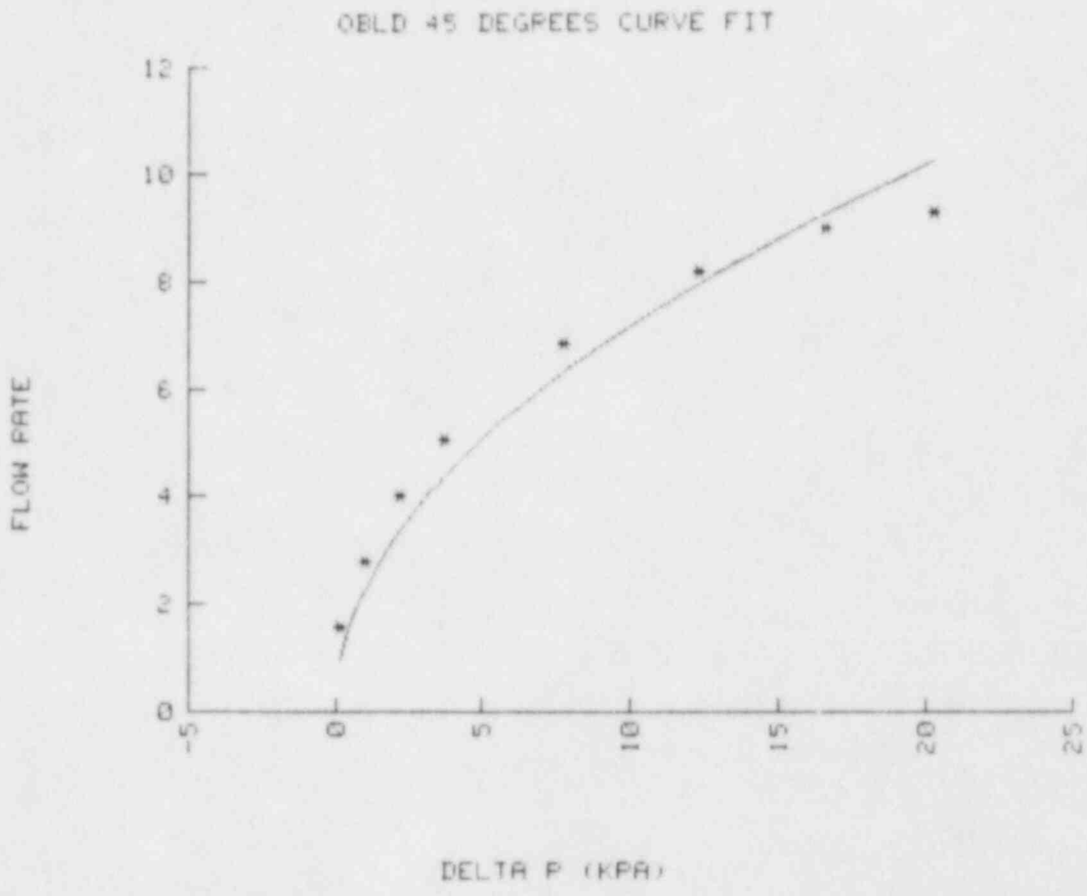
OBLD 45 DEGREES CURVE FIT
FLOW RATE
DELTA P (KPA)
12
10
8
6
4
2
0
-5
0
5
10
15
20
25

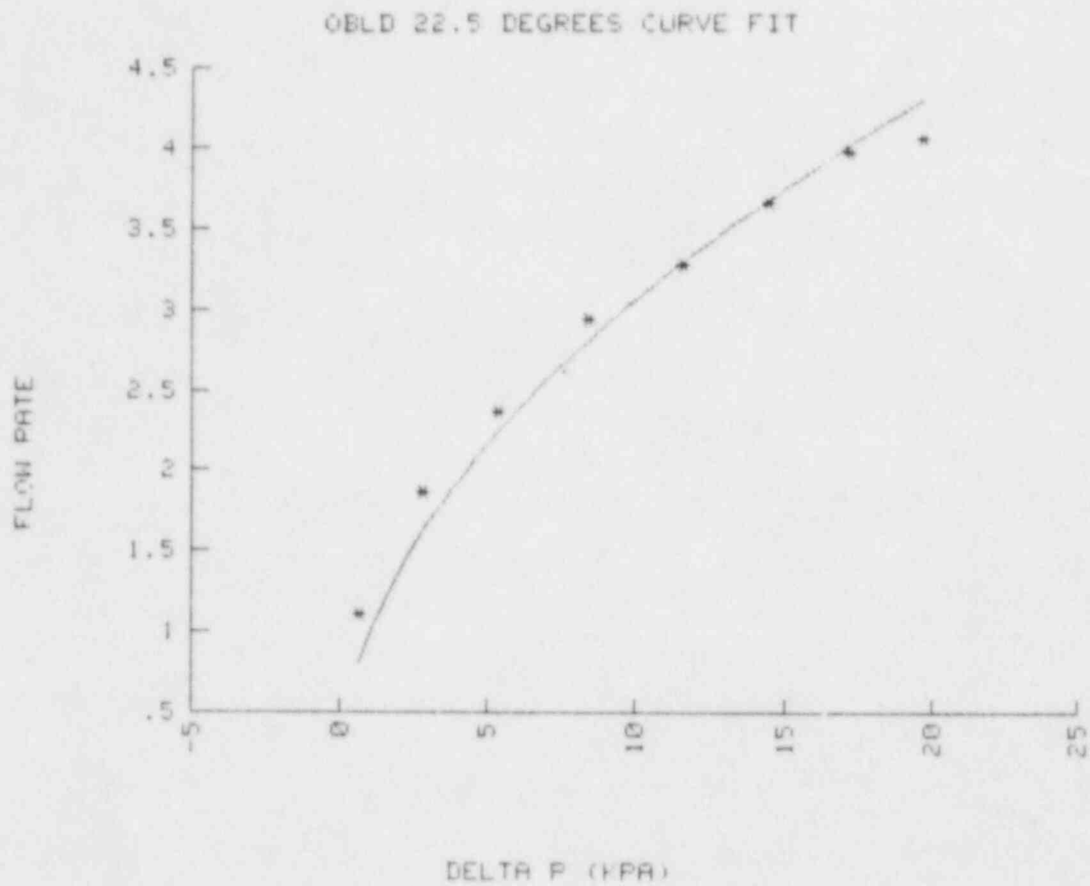

OBLD 22.5 DEGREES CURVE FIT
FLOW RATE
DELTA P (KPA)
4.5
4
3.5
3
2.5
2
1.5
1
.5
-5
0
5
10
15
20
25

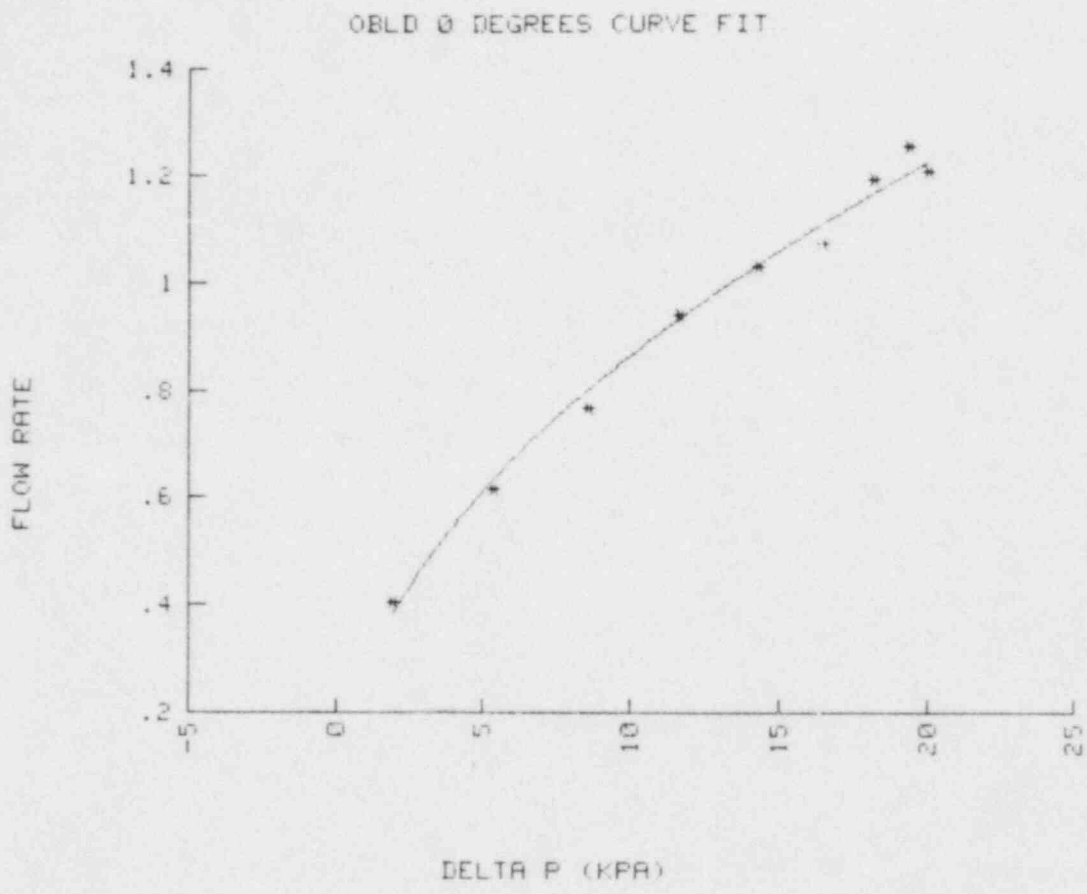
OBLD Ø DEGREES CURVE FIT
FLOW RATE
1.4
1.2
1
.8
.6
.4
.2
-5
0
5
10
15
20
25
DELTA P (KPA)

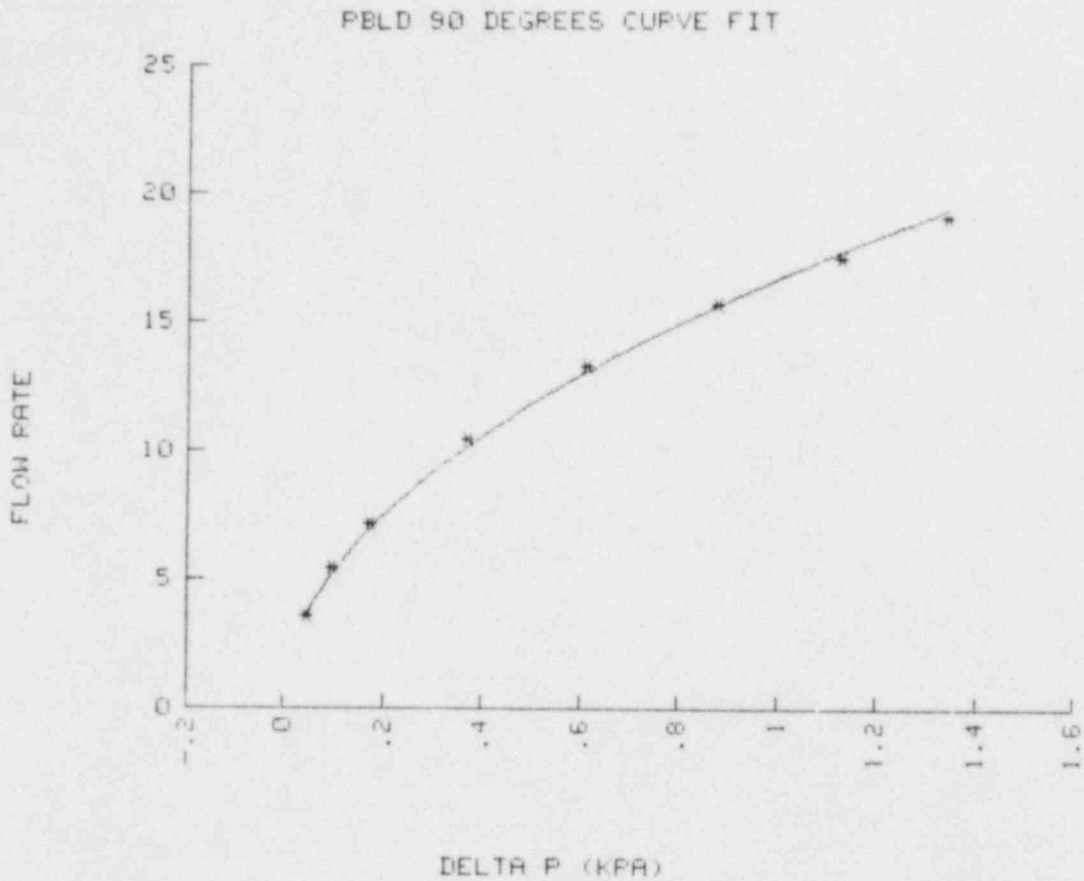
PBLD 90 DEGREES CURVE FIT
FLOW RATE
DELTA P (KPA)
25
20
15
10
5
0
-.2
0
.2
.4
.6
.8
1
1.2
1.4
1.6

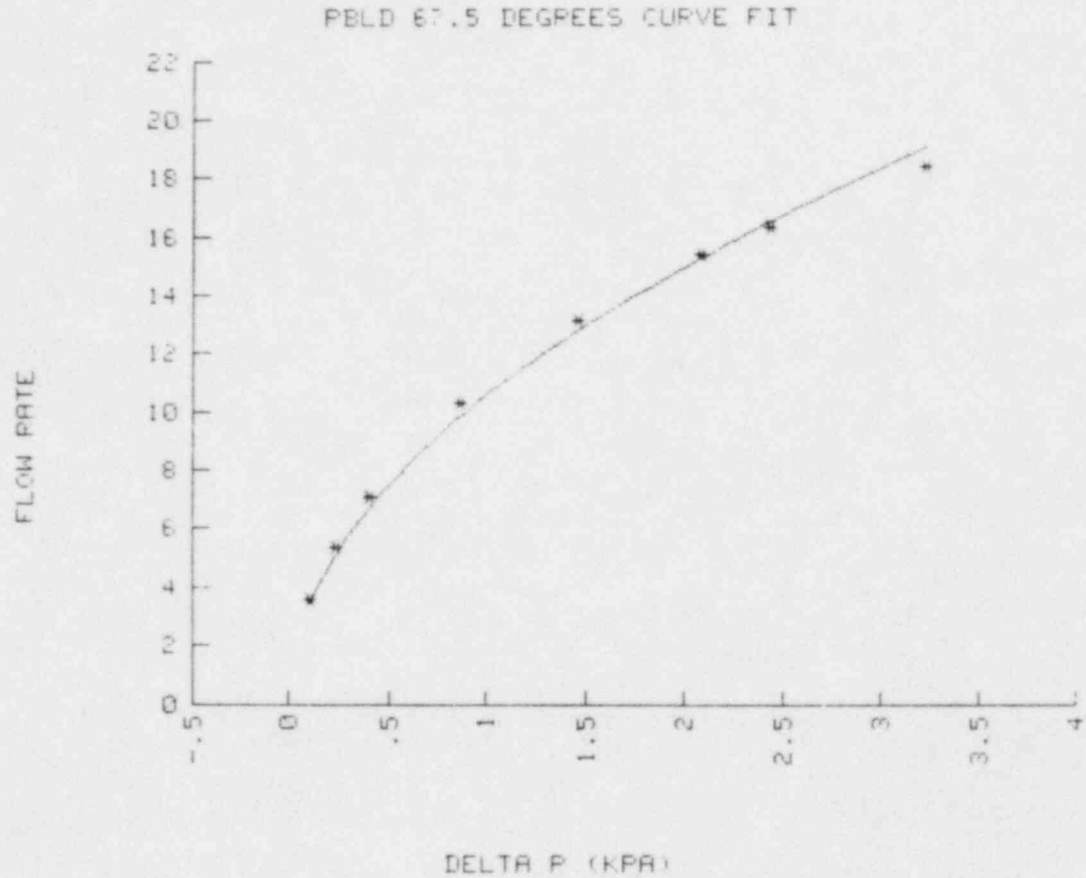
PBLD 67.5 DEGREES CURVE FIT
FLOW RATE
DELTA P (KPA)
0
2
4
6
8
10
12
14
16
18
20
22
-.5
0
.5
1
1.5
2
2.5
3
3.5
4

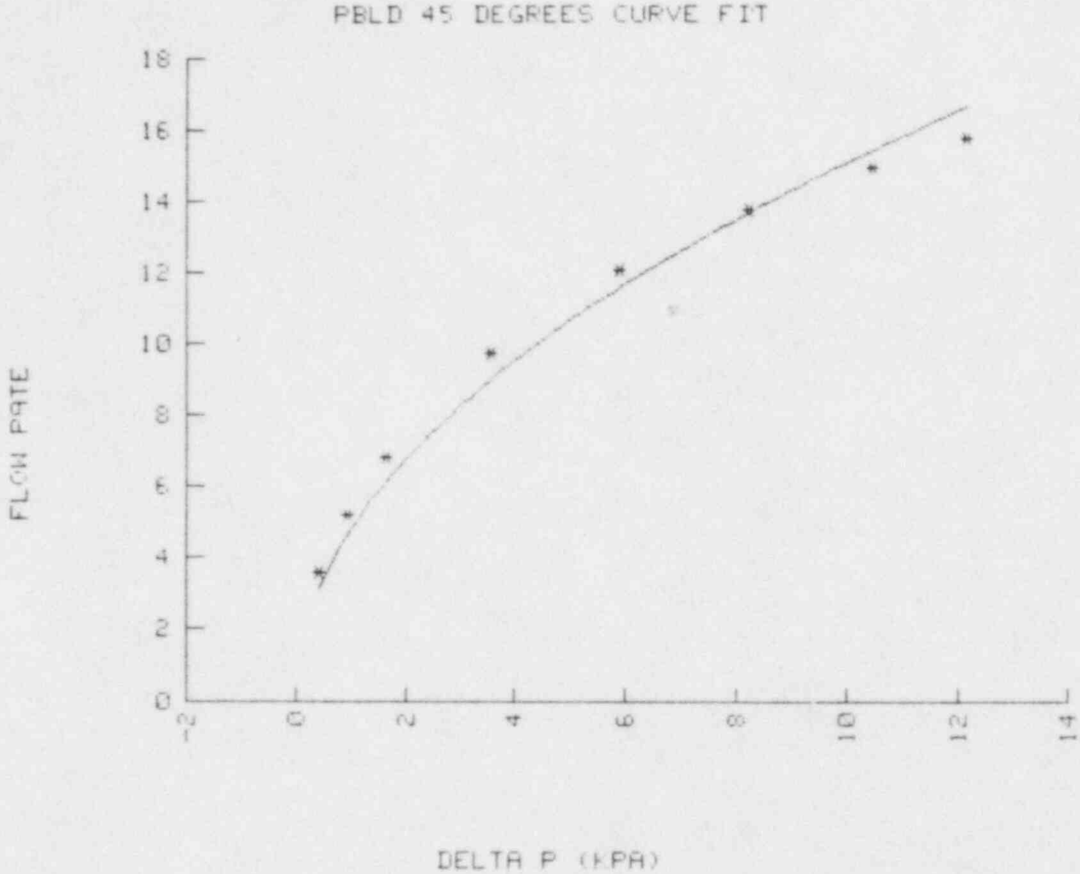
PBLD 45 DEGREES CURVE FIT
FLOW RATE
DELTA P (KPA)
18
16
14
12
10
8
6
4
2
0
-2
0
2
4
6
8
10
12
14

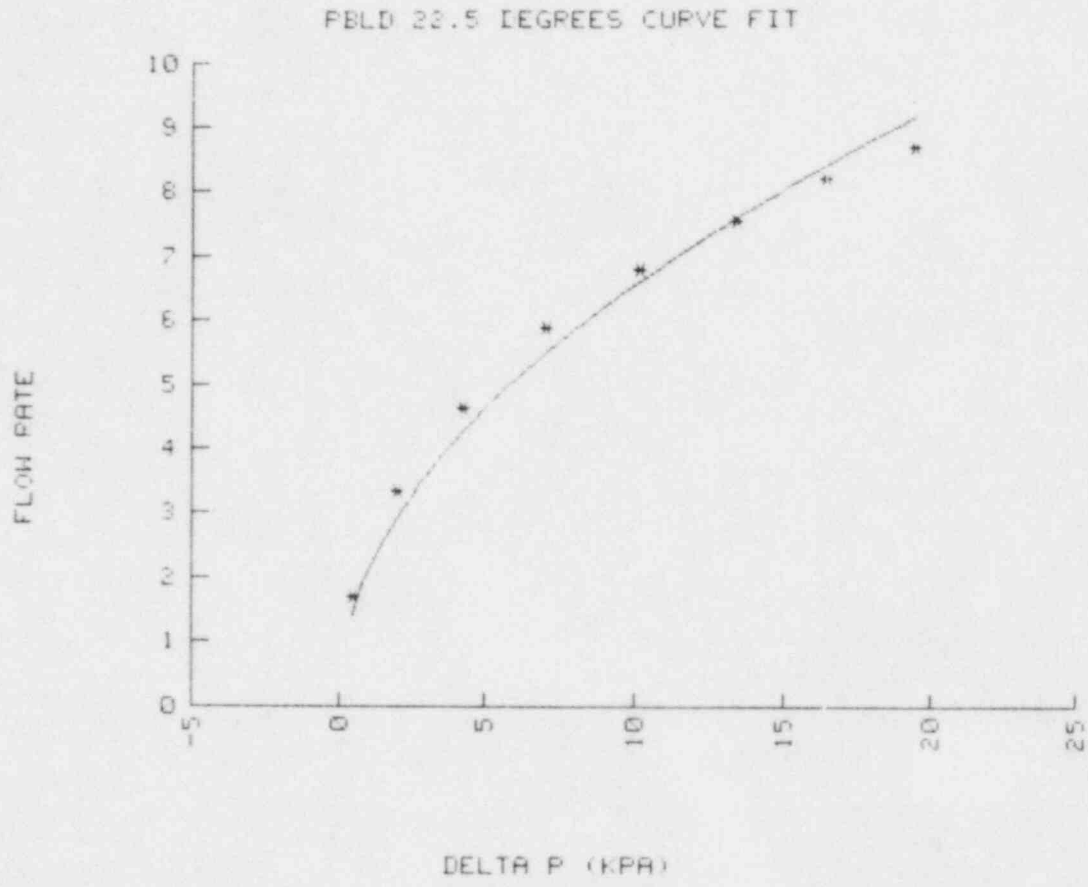

PBLD 22.5 DEGREES CURVE FIT
FLOW RATE
DELTA P (KPA)
0
1
2
3
4
5
6
7
8
9
10
-5
0
5
10
15
20
25

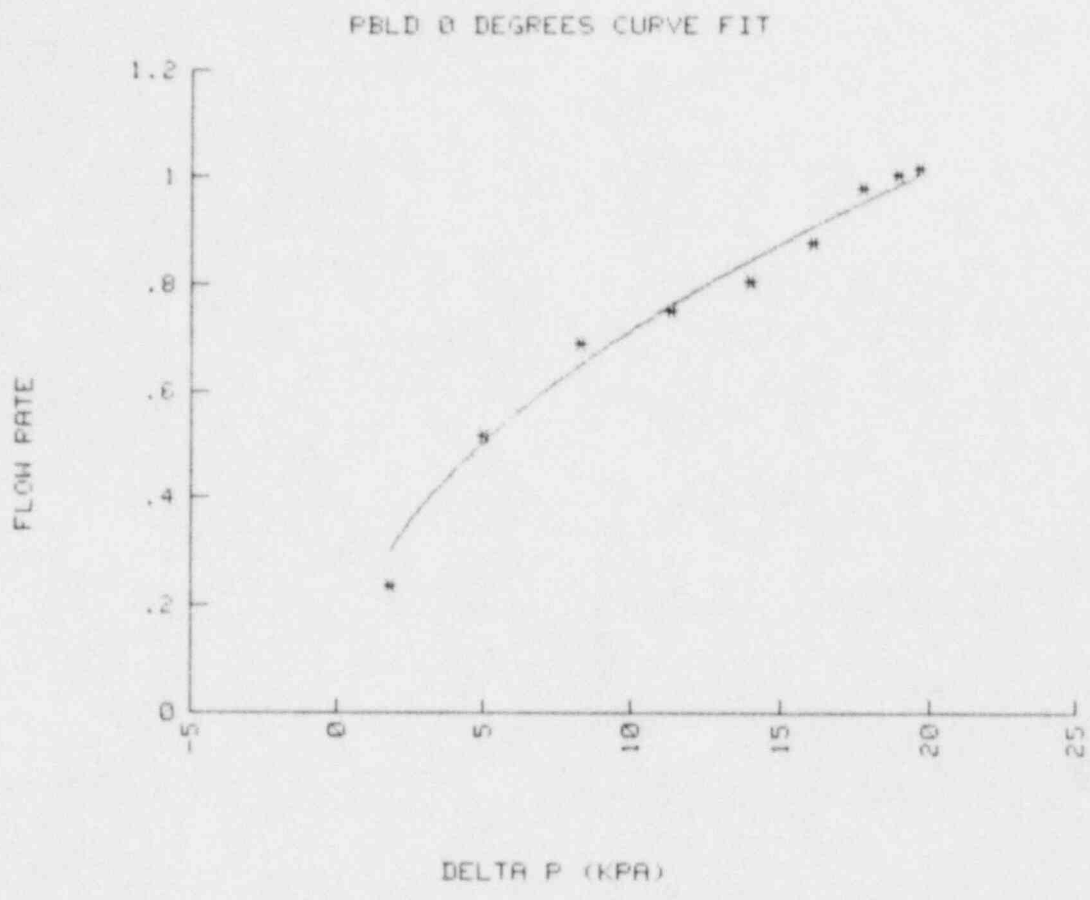
PBLD 0 DEGREES CURVE FIT
FLOW RATE
DELTA P (KPA)
1.2
1
.8
.6
.4
.2
0
-5
0
5
10
15
20
25

DISTRIBUTION

	Copies
Nuclear Regulatory Commission, RD, Bethesda, Maryland	273
Technical Information Center, Oak Ridge, Tennessee	2
Los Alamos National Laboratory, Los Alamos, New Mexico	38
	313

☆ U.S. GOVERNMENT PRINTING OFFICE 1985—576-034/20061

NRC FORM 335 (2-84) NRCM 1102, 3201, 3202

U.S. NUCLEAR REGULATORY COMMISSION

BIBLIOGRAPHIC DATA SHEET

SEE INSTRUCTIONS ON THE REVERSE

1. REPORT NUMBER (Assigned by TIDC add Vol. No., if any)
NUREG/CR-4232
LA-10413-MS

2. TITLE AND SUBTITLE
The Response of Ventilation Dampers to Large Airflow Pulses

3. LEAVE BLANK

4. DATE REPORT COMPLETED

MONTH	YEAR
April	1985

5. AUTHOR(S)
W. S. Gregory and P. R. Smith

6. DATE REPORT ISSUED

MONTH	YEAR
April	1985

7. PERFORMING ORGANIZATION NAME AND MAILING ADDRESS (Include Zip Code)
Los Alamos National Laboratory
Los Alamos, NM 87545

8. PROJECT/TASK/WORK UNIT NUMBER

9. FIN OR GRANT NUMBER
A7028

10. SPONSORING ORGANIZATION NAME AND MAILING ADDRESS (Include Zip Code)
Division of Risk Analysis
Office of Nuclear Regulatory Research
U.S. Nuclear Regulatory Commission
Washington, DC 20555

11a. TYPE OF REPORT
Informal

b. PERIOD COVERED (Inclusive dates)

12. SUPPLEMENTARY NOTES

13. ABSTRACT (200 words or less)
The results of an experimental program to evaluate the response of ventilation system dampers to simulated tornado transients are reported. Relevant data, such as damper response time, flow rate and pressure drop, and flow/pressure vs blade angle, were obtained, and the response of one tornado protective damper to simulated tornado transients was evaluated. Empirical relationships that will allow the data to be integrated into flow dynamics codes were developed. These flow dynamics codes can be used by safety analysts to predict the response of nuclear facility ventilation systems to tornado depressurizations.

14. DOCUMENT ANALYSIS - a. KEYWORDS/DESCRIPTORS

b. IDENTIFIERS/OPEN-ENDED TERMS

15. AVAILABILITY STATEMENT
Unlimited

16. SECURITY CLASSIFICATION
(This page)
Unclassified
(This report)
Unclassified

17. NUMBER OF PAGES

18. PRICE

Available from

GPO Sales Program
Division of Technical Information and Document Control
US Nuclear Regulatory Commission
Washington, DC 20555

and

National Technical Information Service
Springfield, VA 22161

Los Alamos